

# POD-Galerkin Model Order Reduction for Parametrized Nonlinear Time Dependent Optimal Flow Control: an Application to Shallow Water Equations.

Maria Strazzullo<sup>#</sup>, Francesco Ballarin<sup>#</sup>, and Gianluigi Rozza<sup>#</sup>

<sup>#</sup>*mathlab, Mathematics Area, International School for Advanced Studies (SISSA), Via Bonomea 265, I-34136 Trieste, Italy.*

maria.strazzullo@sissa.it, francesco.ballarin@sissa.it, gianluigi.rozza@sissa.it

## Abstract

In this work we propose reduced order methods as a reliable strategy to efficiently solve parametrized optimal control problems governed by shallow waters equations in a solution tracking setting. The physical parametrized model we deal with is nonlinear and time dependent: this leads to very time consuming simulations which can be unbearable e.g. in a marine environmental monitoring plan application. Our aim is to show how reduced order modelling could help in studying different configurations and phenomena in a fast way. After building the optimality system, we rely on a POD-Galerkin reduction in order to solve the optimal control problem in a low dimensional reduced space. The presented theoretical framework is actually suited to general nonlinear time dependent optimal control problems. The proposed methodology is finally tested with a numerical experiment: the reduced optimal control problem governed by shallow waters equations reproduces the desired velocity and height profiles faster than the standard model, still remaining accurate.

## 1 Introduction

Parametrized optimal control problems (OCP( $\mu$ )s) governed by parametrized partial differential equations (PDE( $\mu$ )s) are very powerful mathematical formulations, to be exploited in several applications in different scientific fields, see [39] for an overview. Among the possible impact that OCP( $\mu$ )s can have in scientific research, we will refer to the investigation into problems dealing with environmental sciences applications. Indeed, this work is motivated by the ongoing demand for reaching fast and accurate simulations for the coastal marine environment safeguard. The marine ecosystem is linked to other important social factors such as, for example, economic growth, natural resources preservation, monitoring plans. Furthermore, the marine environment is very far to be completely understood, since it is linked to very complicated natural phenomena and anthropic consequences [18, 45, 56].

For sure, the parametric setting is necessary in order to study different configurations: the parameter  $\mu \in \mathcal{P} \subset \mathbb{R}^d$  could represent a variety of physical phenomena. Moreover, in the environmental field, the theory of OCP( $\mu$ )s fits well with the need of increasing the models forecast capabilities through a data assimilation approach [26, 33, 66]. A lot of effort is made in order to make PDEs models based predictions the most similar to collected data. Data assimilation OCP( $\mu$ )s have been already analysed in several works, as [21, 49, 50, 61, 63]. Yet, the main drawback of data assimilated problems is the huge computational complexity which still limits their applicability, most of all if the optimization problem deals with very complicated

parametric flow models, as the ones used in marine and coastal engineering. Furthermore, in the described context, accurate simulations are required in a small amount of time, in order to better study and analyse them: indeed, the primal goal is to manage different situations. This is the reason that motivates the use of Reduced Order Methods (ROMs) as a suitable approach for rapid and accurate surrogate simulations of partial differential equations PDE( $\mu$ )s [27, 48, 53]. The main feature of ROM techniques is to solve the parametrized problem in a low dimensional framework in order to save computational resources which can be exploited for the analysis of several parametric configurations: ROMs recast a time consuming simulation, the *truth problem*, into a new fast and reliable formulation thanks to a Galerkin projection into reduced spaces, generated by basis functions derived from a proper orthogonal decomposition (POD) algorithm, as presented in [9, 16, 19, 27].

In general, reduction methods for parametrized nonlinear time dependent OCP( $\mu$ )s are very complex to analyse both theoretically and numerically. Although the literature is quite consolidated for steady constraints, see for example [7, 8, 20, 25, 34, 36, 37, 47, 46, 50], where the interested reader may find theoretical and numerical analysis for different linear models, there is very small knowledge about time dependency [31, 35, 61, 63]. Another difficulty to be overcome is the treatment and the reduction of nonlinear OCP( $\mu$ )s, see for example [38, 54, 61, 63, 71].

In this work, we focus on ROM for OCP( $\mu$ )s with quadratic cost functional constrained to parametrized Shallow Waters Equations (SWEs). The latter is a very useful model in environmental sciences, which is capable to simulate various marine phenomena such as, for example, tidal flows and mixing, currents action on shores and coasts, planetary flows and even tsunamis [18, 68]. The state equation proposed is nonlinear and time dependent: this leads to growing complexity in the solution of the optimality system in a real-time context. Indeed, even if the state equation and the control problem have been analysed and managed numerically with many approaches, see for example [2, 3, 4, 5, 24, 44, 43, 42, 51, 52, 64], their parametric formulation is still quite unexplored and based on time reduction of the state equation [57, 58].

The main novelty of this work is to perform reduction on the parametric space on the complete SWEs model, i.e nonlinear and time dependent, in a solution tracking optimal control framework. We aim at making a further step towards forecasting data assimilated coastal models which could be used as resources to manage realistic experiments involved in marine sciences with environmental prevision purposes. Indeed, ROMs could be very effective in providing a large number of parametric simulations in an acceptable amount of time, and this can be very useful in order to understand better the considered physical phenomenon. Moreover, we extend the standard reduced techniques for OCP( $\mu$ )s, already exploited for steady and time dependent linear problems, in order to deal with nonlinear state equations. We will show how ROM could be a good strategy which will give us faster, but still accurate, results.

The work is outlined as follows. In Section 2, we first present the SWEs model and then we show it in the optimal control framework. Moreover, we briefly describe the Finite Element approximation and the algebraic version of the presented solution tracking problem. Section 3 will introduce the basic ideas behind ROM discretization for OCP( $\mu$ )s [27, 32, 34]: we will describe POD sampling algorithm for OCP( $\mu$ )s and the aggregated reduced spaces technique used in [20, 46, 47] which will guarantee the solvability of the optimality system in its saddle point formulation. Moreover, we will briefly mention affine decomposition assumption, see e.g. [27], needed for an efficient solve of the reduced system. In Section 4, we test our methodology on a parametrized OCP( $\mu$ )s governed by the SWE equations, inspired by an uncontrolled numerical test case of [24], where the evolution a Gaussian water height is studied. Our test case aims at recovering a given desired velocity-height profile. Finally, conclusions and perspectives follow in Section 5.

## 2 Problem Formulation and Discretization

In this section, we will introduce a OCP( $\mu$ ) governed by SWEs and its truth discretization. As already mentioned in Section 1, the SWEs are a great tool in order to simulate coastal behaviour. A brief introduction to the state equation follows. Then, the SWEs will be connected to their OCP( $\mu$ ) framework in Section 2.2. Then, we will describe the full order approximation of our problem based on the Finite Element approach.

### 2.1 The Shallow Waters Equations

Now we aim at describing the parametrized SWEs. The interested reader may refer to classical references [18, 68], where the topic is deeply analysed in its total generality for a space-time domain  $Q = \Omega \times (0, T) \subset \mathbb{R}^2 \times \mathbb{R}$ . This state equation has been studied both from the analytical and numerical point of view in many works, see, for example, [2, 3, 4, 24, 44, 43, 42, 51, 52]. Let us define  $Y_v = H_{\Gamma_{D_v}}^1(\Omega)$ ,  $Y_h = L_{\Gamma_{D_h}}^2(\Omega)$  and the space  $U = [L^2(\Omega)]^2$ , where  $\Gamma_{D_v}$  and  $\Gamma_{D_h}$  are portions of the boundary domain  $\partial\Omega$  where Dirichlet boundary conditions have been imposed for the vertically averaged velocity profile of the wave  $\mathbf{v}$  and the free surface elevation variable  $h$ , respectively. With the term  $\eta = h - z_b$  we indicate the water depth, where  $z_b$  represents the bottom bathymetry of the domain that we are considering: a schematic description of the involved variables is given by Figure 1. We used the standard 2D-model obtaining by the vertical integration of the velocity variable as presented in [3, 44].

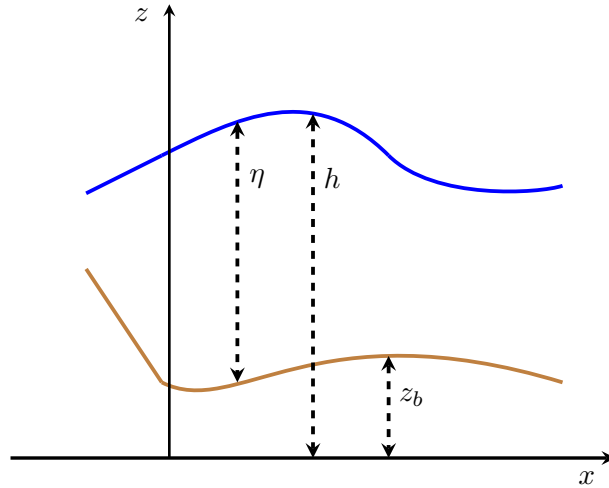


**Figure 1:** Notations: schematic representation.

Since we are dealing with time dependent problems, we seek our state solution in the spaces

$$\mathcal{Y}_v = \left\{ \mathbf{v} \in L^2(0, T; [Y_v]^2) \text{ such that } \frac{\partial \mathbf{v}}{\partial t} \in L^2(0, T; [Y_v^*]^2) \right\},$$

and similarly in

$$\mathcal{Y}_h = \left\{ h \in L^2(0, T; Y_h) \text{ such that } \frac{\partial h}{\partial t} \in L^2(0, T; Y_h^*) \right\},$$

for velocity and height variables, respectively.

We will denote by  $\mathcal{Y}$  the product of the function spaces  $\mathcal{Y}_v$  and  $\mathcal{Y}_h$ , i.e.  $\mathcal{Y} = \mathcal{Y}_v \times \mathcal{Y}_h$ . Moreover,

$\mathcal{Y}$  is an Hilbert space with the following norm:

$$\|(\star, \cdot)\|_{\mathcal{Y}}^2 = \|\star\|_{\mathcal{Y}_v}^2 + \|\cdot\|_{\mathcal{Y}_h}^2 = \|\star\|_{L^2(0,T;[Y_v]^2)}^2 + \left\| \frac{\partial \star}{\partial t} \right\|_{L^2(0,T;[Y_v^*]^2)}^2 + \|\cdot\|_{L^2(0,T;Y_h)}^2 + \left\| \frac{\partial \cdot}{\partial t} \right\|_{L^2(0,T;Y_h^*)}^2.$$

We considered a SWEs model with the following parametrized formulation: given  $\boldsymbol{\mu} \in \Theta \subset \mathbb{R}^2$  and a forcing term  $\mathbf{u} \in \mathcal{U} := L^2(0, T; U)$ , find the parameter dependent pair  $(\mathbf{v}, h) \in \mathcal{Y}$  which satisfies:

$$\begin{cases} \frac{\partial \mathbf{v}}{\partial t} + \mu_1 \Delta \mathbf{v} + \mu_2 (\mathbf{v} \cdot \nabla) \mathbf{v} + g \nabla \eta - \mathbf{u} = 0 & \text{in } Q, \\ \frac{\partial h}{\partial t} + \operatorname{div}(\eta \mathbf{v}) = 0 & \text{in } Q, \\ \mathbf{v} = \mathbf{v}_0 & \text{on } \Omega \times \{0\}, \\ h = h_0 & \text{on } \Omega \times \{0\}, \\ \mathbf{v} = \mathbf{0} & \text{on } \partial\Omega \times [0, T]. \end{cases} \quad (1)$$

We stress that the solution depends on the parameter  $\boldsymbol{\mu} = (\mu_1, \mu_2)$ , i.e.  $(\mathbf{v}, h) := (\mathbf{v}(\boldsymbol{\mu}), h(\boldsymbol{\mu}))$ , but in the following we will omit such dependence for compactness of notation. The proposed analysis does not change with other general boundary conditions: for an insight on the admissible boundary conditions we refer to [4]. The proposed model describes free surface incompressible flows under the assumption of hydrostatic pressure. This hypothesis is valid when the water height is much lower than the wavelength: this is the case of coastal behaviour and shallow depths. In equation (1), we simplistically represent with the forcing term  $\mathbf{u}$  all the physical quantities which can affect the dynamic of the solution, such as the wind stress and the bottom friction: the reason of this choice will be clarified in the next Section. Moreover, we deal with the following parametric context:  $\mu_1$  and  $\mu_2$  represent how diffusion and advection phenomena affect the shallow waters system, respectively. Furthermore, we assume the bottom to be constant with respect to time and spatial variables for simplicity. Indeed, under this assumption, the bottom has no influence on the system considered, since:

$$\nabla \eta = \nabla h \text{ and } \operatorname{div}(\eta \mathbf{v}) = \operatorname{div}(h \mathbf{v}) - \underbrace{z_b \operatorname{div}(\mathbf{v})}_{=0} = \operatorname{div}(h \mathbf{v}).$$

In the next Section, we propose an optimal control problem governed by SWEs, briefly introducing Lagrangian formulation and derivation of the optimality system.

## 2.2 Optimal control problem governed by Shallow Waters Equations

In this Section we are going to introduce a time dependent OCP( $\boldsymbol{\mu}$ ) governed by parametrized SWEs. This Section will combine the state equation (1) to a minimization problem. The goal is to link the optimal control theory coupled with SWEs coastal water model as a powerful instrument in order to manage marine monitoring issues.

Theoretically, we will follow the general theory for time dependent OCP( $\boldsymbol{\mu}$ ) proposed in [65, chapter 3]. In Section 2.1 we already introduced the *state variable*  $(\mathbf{v}, h) \in \mathcal{Y}$ . In order to set up an OCP( $\boldsymbol{\mu}$ ) we need to define a *control variable*  $\mathbf{u}$  in the function space  $\mathcal{U}$ . In our applications, we deal with a distributed optimal control, i.e., the control variable represents the forcing term representing the wind action, atmospheric pressure and to the bottom slope effect. Then, even if we are not actually controlling the system, the optimal control framework can be interpreted as an inverse problem which specifies the physical conditions guaranteeing a desired velocity-height profile  $(\mathbf{v}_d, h_d) \in \mathcal{Y}$ . Let us define the *state-control variable*  $x = ((\mathbf{v}, h), \mathbf{u}) \in \mathcal{X} = \mathcal{Y} \times \mathcal{U}$ . As



already stressed in the previous Section, even if the variables are  $\boldsymbol{\mu}$ -dependent, for the sake of notation we will use  $((\mathbf{v}, h), \mathbf{u}) := ((\mathbf{v}(\boldsymbol{\mu}), h(\boldsymbol{\mu})), \mathbf{u}(\boldsymbol{\mu}))$  and  $x := x(\boldsymbol{\mu})$ .

We deal with parametrized SWEs: our optimal control problem depends on a physical parameter  $\boldsymbol{\mu} = (\mu_1, \mu_2, \mu_3)$  in the parameter space  $\mathcal{P} \subset \mathbb{R}^3$ . The role of parameter  $\mu_1$  and  $\mu_2$  was already introduced in Section 2.1, while the component  $\mu_3$  affects the desired solution profile.

The parametrized OCP( $\boldsymbol{\mu}$ ) has the following formulation: given a parameter  $\boldsymbol{\mu} \in \mathcal{P}$ , find  $x(\boldsymbol{\mu}) \in \mathcal{X}$  which solves  $\min_{x(\boldsymbol{\mu}) \in \mathcal{X}} J(x(\boldsymbol{\mu}))$  under the constraint (1) with

$$J(x(\boldsymbol{\mu})) = \frac{1}{2} \int_0^T \int_{\Omega} (h - h_d(\mu_3))^2 d\Omega dt + \frac{1}{2} \int_0^T \int_{\Omega} (\mathbf{v} - \mathbf{v}_d(\mu_3))^2 d\Omega dt + \frac{\alpha}{2} \int_0^T \int_{\Omega} \mathbf{u}^2 d\Omega dt, \quad (2)$$

where  $\alpha \in (0, 1]$  is a penalization parameter.

In order to solve the problem, we exploit a Lagrangian approach which allowed us to build the optimality conditions that will be discretized in the following sections: in other words we applied an *optimize-then-discretize* strategy, which first derives the optimality system at the continuous level and approximates it only at the end of the procedure as presented in [23]. First of all, our problem can be recast in the following weak formulation: given a parameter  $\boldsymbol{\mu} \in \mathcal{P}$ , find  $x(\boldsymbol{\mu}) \in \mathcal{X}$  which minimizes (2) such that the weak state equation  $\mathcal{S}(x, (\boldsymbol{\kappa}, \xi); \boldsymbol{\mu}) = 0$  is verified for all  $(\boldsymbol{\kappa}, \xi) \in \mathcal{Y}$ , where  $\mathcal{S}(x, (\boldsymbol{\kappa}, \xi); \boldsymbol{\mu}) = 0$  reads as follows:

$$\begin{cases} \int_0^T \int_{\Omega} \frac{\partial \mathbf{v}}{\partial t} \cdot \boldsymbol{\kappa} d\Omega dt + \mu_1 a_1((\mathbf{v}, h), (\boldsymbol{\kappa}, \xi)) + \mu_2 \int_0^T a_1^{\text{nl}}((\mathbf{v}, h), (\mathbf{v}, h), (\boldsymbol{\kappa}, \xi)) dt \\ \quad + \int_0^T a_2((\mathbf{v}, h), (\boldsymbol{\kappa}, \xi)) dt = \int_0^T \int_{\Omega} \mathbf{u} \cdot \boldsymbol{\kappa} d\Omega dt & \forall (\boldsymbol{\kappa}, \xi) \in \mathcal{Y}, \\ \int_0^T \int_{\Omega} \frac{\partial h}{\partial t} \xi d\Omega dt + \int_0^T a_2^{\text{nl}}((\mathbf{v}, h), (\mathbf{v}, h), (\boldsymbol{\kappa}, \xi)) dt = 0 & \forall (\boldsymbol{\kappa}, \xi) \in \mathcal{Y}, \end{cases} \quad (3)$$

and  $a_1(\cdot, \cdot), a_2(\cdot, \cdot), a_1^{\text{nl}}(\cdot, \cdot, \cdot), a_2^{\text{nl}}(\cdot, \cdot, \cdot)$  are defined as follows:

$$\begin{aligned} a_1 : \mathcal{Y} \times \mathcal{Y} &\rightarrow \mathbb{R} & a_1((\mathbf{v}, h), (\boldsymbol{\kappa}, \xi)) &= \int_{\Omega} \nabla \mathbf{v} : \nabla \boldsymbol{\kappa} d\Omega, \\ a_2 : \mathcal{Y} \times \mathcal{Y} &\rightarrow \mathbb{R} & a_2((\mathbf{v}, h), (\boldsymbol{\kappa}, \xi)) &= \int_{\Omega} g \boldsymbol{\kappa} : \nabla h d\Omega, \\ a_1^{\text{nl}} : \mathcal{Y} \times \mathcal{Y} \times \mathcal{Y} &\rightarrow \mathbb{R} & a_1^{\text{nl}}((\mathbf{v}, h), (\mathbf{w}, \varphi), (\boldsymbol{\kappa}, \xi)) &= \int_{\Omega} \boldsymbol{\kappa} : (\mathbf{v} \cdot \nabla) \mathbf{w} d\Omega, \\ a_2^{\text{nl}} : \mathcal{Y} \times \mathcal{Y} \times \mathcal{Y} &\rightarrow \mathbb{R} & a_2^{\text{nl}}((\mathbf{v}, h), (\mathbf{w}, \varphi), (\boldsymbol{\kappa}, \xi)) &= \int_{\Omega} \xi \operatorname{div}(\varphi \mathbf{v}) d\Omega. \end{aligned}$$

We have specified the nonlinear nature of the involved quantities with an “nl” as apex. Moreover, we introduce an adjoint variable  $(\boldsymbol{\chi}, \lambda) := (\boldsymbol{\chi}(\boldsymbol{\mu}), \lambda(\boldsymbol{\mu})) \in \mathcal{Y}$ . Now we have all the elements in order to build the following Lagrangian functional

$$\mathcal{L}((\mathbf{v}, h), \mathbf{u}, (\boldsymbol{\chi}, \lambda)) = J(x) + \mathcal{S}(x, (\boldsymbol{\chi}, \lambda); \boldsymbol{\mu}). \quad (4)$$

In order to solve the constrained minimization of (2), we differentiate with respect to the variables  $((\mathbf{v}, h), \mathbf{u}, (\boldsymbol{\chi}, \lambda))$  obtaining the following system to be solved:

$$\begin{cases} D_{\mathbf{v}} \mathcal{L}((\mathbf{v}, h), \mathbf{u}, (\boldsymbol{\chi}, \lambda))[z] = 0 & \forall z \in \mathcal{Y}_v, \\ D_h \mathcal{L}((\mathbf{v}, h), \mathbf{u}, (\boldsymbol{\chi}, \lambda))[q] = 0 & \forall q \in \mathcal{Y}_h, \\ D_{\mathbf{u}} \mathcal{L}((\mathbf{v}, h), \mathbf{u}, (\boldsymbol{\chi}, \lambda))[\boldsymbol{\tau}] = 0 & \forall \boldsymbol{\tau} \in \mathcal{U}, \\ D_{\boldsymbol{\chi}} \mathcal{L}((\mathbf{v}, h), \mathbf{u}, (\boldsymbol{\chi}, \lambda))[\boldsymbol{\kappa}] = 0 & \forall \boldsymbol{\kappa} \in \mathcal{Y}_v, \\ D_{\lambda} \mathcal{L}((\mathbf{v}, h), \mathbf{u}, (\boldsymbol{\chi}, \lambda))[\xi] = 0 & \forall \xi \in \mathcal{Y}_h. \end{cases} \quad (5)$$

The differentiation with respect to the adjoint variable  $(\chi, \lambda)$  coincides with the *state equation*. Moreover, differentiation with respect to the control variable  $\mathbf{u}$  leads to the *optimality equation*, which has the following form:

$$\alpha \int_0^T \int_{\Omega} \mathbf{u} \cdot \boldsymbol{\tau} \, d\Omega dt = \int_0^T \int_{\Omega} \chi \cdot \boldsymbol{\tau} \, d\Omega dt \quad \forall \boldsymbol{\tau} \in \mathcal{U}.$$

Finally, we can derive the *adjoint equation*, which reads as:

$$\left\{ \begin{array}{l} \int_0^T \int_{\Omega} \mathbf{v} \cdot \mathbf{z} \, d\Omega dt - \int_0^T \int_{\Omega} \frac{\partial \chi}{\partial t} \cdot \mathbf{z} \, d\Omega dt + \mu_1 \int_0^T a_1^*((\chi, \lambda), (\mathbf{z}, q)) \, dt \\ \quad + \mu_2 \int_0^T a_1^{\text{nl}*}((\mathbf{v}, h), (\chi, \lambda), (\mathbf{z}, q)) \, dt \\ \quad + \int_0^T a_2^{\text{nl}*}((\mathbf{v}, h), (\chi, \lambda), (\mathbf{z}, q)) \, dt = \int_0^T \int_{\Omega} \mathbf{v}_d \cdot \mathbf{z} \, d\Omega dt \quad \forall (\mathbf{z}, q) \in \mathcal{Y}, \\ \int_0^T \int_{\Omega} h q \, d\Omega dt - \int_0^T \int_{\Omega} \frac{\partial h}{\partial t} q \, d\Omega dt + \int_0^T a_3^{\text{nl}*}((\mathbf{v}, h), (\chi, h), (\mathbf{z}, q)) \, dt \\ \quad + \int_0^T a_3^*((\chi, \lambda), (\mathbf{z}, q)) \, dt = \int_0^T \int_{\Omega} h_d q \, d\Omega dt \quad \forall (\mathbf{z}, q) \in \mathcal{Y}, \end{array} \right. \quad (6)$$

where the involved forms are defined as

$$\begin{aligned} a_1^* &\equiv a_1 : \mathcal{Y} \times \mathcal{Y} \rightarrow \mathbb{R} & a_1((\chi, \lambda), (\mathbf{z}, q)) &= \int_{\Omega} \nabla \chi : \nabla \mathbf{z} \, d\Omega, \\ a_1^{\text{nl}*} &: \mathcal{Y} \times \mathcal{Y} \times \mathcal{Y} \rightarrow \mathbb{R} & a_1^{\text{nl}*}((\mathbf{v}, h), (\chi, \lambda), (\mathbf{z}, q)) &= - \int_{\Omega} (\mathbf{v} \cdot \nabla) \chi \cdot \mathbf{z} \, d\Omega + \int_0^T \int_{\Omega} (\nabla \mathbf{v})^T \chi \cdot \mathbf{z} \, d\Omega dt, \\ a_2^{\text{nl}*} &: \mathcal{Y} \times \mathcal{Y} \times \mathcal{Y} \rightarrow \mathbb{R} & a_2^{\text{nl}*}((\mathbf{v}, h), (\chi, \lambda), (\boldsymbol{\kappa}, \xi)) &= - \int_{\Omega} h \nabla \lambda \cdot \mathbf{z} \, d\Omega, \\ a_3^{\text{nl}*} &: \mathcal{Y} \times \mathcal{Y} \times \mathcal{Y} \rightarrow \mathbb{R} & a_3^{\text{nl}*}((\mathbf{v}, h), (\chi, \lambda), (\mathbf{z}, q)) &= - \int_{\Omega} \mathbf{v} \cdot \nabla \lambda q \, d\Omega, \\ a_3^* &: \mathcal{Y} \times \mathcal{Y} \rightarrow \mathbb{R} & a_3^*((\chi, \lambda), (\mathbf{z}, q)) &= -g \int_{\Omega} \text{div}(\chi) q \, d\Omega. \end{aligned}$$

The just specified weak formulation of (5), corresponds to the following optimality system in strong formulation:

$$\left\{ \begin{array}{ll} \mathbf{v} - \frac{\partial \chi}{\partial t} + \mu_1 \Delta \chi - \mu_2 (\mathbf{v} \cdot \nabla) \chi + \mu_2 (\nabla \mathbf{v})^T \chi - h \nabla \lambda = \mathbf{v}_d & \text{in } Q, \\ h - \frac{\partial \lambda}{\partial t} - \mathbf{v} \cdot \nabla \lambda - g \text{div}(\chi) = h_d & \text{in } Q, \\ \chi = \mathbf{0} & \text{on } \partial\Omega \times (0, T) \\ \chi = \mathbf{0} & \text{on } \Omega \times \{T\}, \\ \lambda = 0 & \text{on } \Omega \times \{T\}, \\ \alpha \mathbf{u} = \chi & \text{in } Q \\ \frac{\partial \mathbf{v}}{\partial t} + \mu_1 \Delta \mathbf{v} + \mu_2 (\mathbf{v} \cdot \nabla) \mathbf{v} + g \nabla h = \mathbf{u} & \text{in } Q, \\ \frac{\partial h}{\partial t} + \text{div}(h \mathbf{v}) = 0 & \text{in } Q, \\ \mathbf{v} = \mathbf{0} & \text{on } \partial\Omega \times (0, T) \\ \mathbf{v} = \mathbf{v}_0 & \text{on } \Omega \times \{0\}, \\ h = h_0 & \text{on } \Omega \times \{0\}. \end{array} \right. \quad (7)$$

We are now able to discretize and solve the system through numerical approximation: in the next Section we propose Finite Element as full order numerical discretization in a all-at-once framework, already presented in [28, 29, 59, 60] for linear and nonlinear constraints.

### 2.3 Finite Element for OCP( $\mu$ )s: All-at-Once Approach

In this Section, we will present the discretization of the OCP( $\mu$ ) defined in Section 2.2. First of all, we will focus on the Finite Element (FE) approximation. The FE discretization is needed for the Reduced Order Model (ROM) approximation, as we will clarify later in Section 3. Indeed, a *truth* problem solution is a necessary step in order to build reduced basis functions to apply model reduction.

Our aim is to build a discretized optimality system based on the *first optimize, then discretize* approach, see e.g. [23]: we first derive the optimality conditions and the equations (7) and then we perform a discretization in time and space through Euler's methods and FE approximation, respectively.

For this purpose, first of all we define a triangulation  $\mathcal{T}$  over our spatial domain  $\Omega$ . We can now provide the FE spaces as  $Y_v^{\mathcal{N}_v} = [Y_v]^2 \cap \mathcal{X}_{r_v}$ ,  $Y_h^{\mathcal{N}_h} = Y_h \cap \mathcal{X}_{r_h}$  and  $U^{\mathcal{N}_u} = U \cap \mathcal{X}_{r_u}$ , where

$$\mathcal{X}_r = \{s^{\mathcal{N}} \in C^0(\bar{\Omega}) : s|_K \in \mathbb{P}^r, \forall K \in \mathcal{T}^{\mathcal{N}}\}.$$

The space  $\mathbb{P}^r$  is the space of all the polynomials of degree at most equal to  $r$  and  $K$  is a triangular element of  $\mathcal{T}$ . Let us refer to  $\mathcal{N}$  as the global FE dimension of the system, i.e.  $\mathcal{N} = 2\mathcal{N}_v + 2\mathcal{N}_h + \mathcal{N}_u$ . Indeed, in this new configuration, the state and adjoint velocity belong to

$$\mathcal{Y}_v^{\mathcal{N}} = \left\{ \mathbf{v} \in L^2(0, T; Y_v^{\mathcal{N}_v}) \text{ such that } \frac{\partial \mathbf{v}}{\partial t} \in L^2(0, T; Y_v^{\mathcal{N}_v*}) \right\},$$

and, similarly, the state and adjoint elevation variables are in the space

$$\mathcal{Y}_h^{\mathcal{N}} = \left\{ h \in L^2(0, T; Y_h^{\mathcal{N}_h}) \text{ such that } \frac{\partial h}{\partial t} \in L^2(0, T; Y_h^{\mathcal{N}_h*}) \right\}.$$

Finally, the function space considered for state and adjoint velocity-height variables is  $\mathcal{Y}^{\mathcal{N}} = \mathcal{Y}_v^{\mathcal{N}} \times \mathcal{Y}_h^{\mathcal{N}}$ , while the control variable is in  $\mathcal{U}^{\mathcal{N}} = L^2(0, T; U^{\mathcal{N}_u})$ . For the sake of notation, we used as apex the global dimension  $\mathcal{N}$  over the spaces, even if it is not the actual dimension of the space considered. Indeed, we are dealing with finite dimensional Hilbert spaces and with the basis functions  $(\{\phi^i\}_{i=1}^{\mathcal{N}_v}, \{\phi^i\}_{i=1}^{\mathcal{N}_h})$  and  $\{\psi^i\}_{i=1}^{\mathcal{N}_u}$  for state/adjoint and control spaces, respectively. The parametrized FE optimality system reads: given  $\mu \in \mathcal{D}$ , find  $((\mathbf{v}^{\mathcal{N}}, h^{\mathcal{N}}), \mathbf{u}^{\mathcal{N}}, (\chi^{\mathcal{N}}, \lambda^{\mathcal{N}}))$  which solves:

$$\begin{cases} D_v \mathcal{L}((\mathbf{v}^{\mathcal{N}}, h^{\mathcal{N}}), \mathbf{u}^{\mathcal{N}}, (\chi^{\mathcal{N}}, \lambda^{\mathcal{N}}))[z] = 0 & \forall z \in \mathcal{Y}_v^{\mathcal{N}}, \\ D_h \mathcal{L}((\mathbf{v}^{\mathcal{N}}, h^{\mathcal{N}}), \mathbf{u}^{\mathcal{N}}, (\chi^{\mathcal{N}}, \lambda^{\mathcal{N}}))[q] = 0 & \forall q \in \mathcal{Y}_h^{\mathcal{N}}, \\ D_u \mathcal{L}((\mathbf{v}^{\mathcal{N}}, h^{\mathcal{N}}), \mathbf{u}^{\mathcal{N}}, (\chi^{\mathcal{N}}, \lambda^{\mathcal{N}}))[\tau] = 0 & \forall \tau \in \mathcal{U}^{\mathcal{N}}, \\ D_\chi \mathcal{L}((\mathbf{v}^{\mathcal{N}}, h^{\mathcal{N}}), \mathbf{u}^{\mathcal{N}}, (\chi^{\mathcal{N}}, \lambda^{\mathcal{N}}))[\kappa] = 0 & \forall \kappa \in \mathcal{Y}_v^{\mathcal{N}}, \\ D_\lambda \mathcal{L}((\mathbf{v}^{\mathcal{N}}, h^{\mathcal{N}}), \mathbf{u}^{\mathcal{N}}, (\chi^{\mathcal{N}}, \lambda^{\mathcal{N}}))[\xi] = 0 & \forall \xi \in \mathcal{Y}_h^{\mathcal{N}}. \end{cases} \quad (8)$$

As we did in Section 2.2, we indicate the state-control variable  $((\mathbf{v}^{\mathcal{N}}, h), \mathbf{u})$  with  $x^{\mathcal{N}}$ . We now deal with the time approximation. The time interval  $(0, T)$  is divided in  $N_t$  equispaced subintervals with  $\Delta t$  as time step. Indeed, at each time  $t_k = k \times \Delta t$  for  $k = 1, \dots, N_t$ , our FE solution variables can be respectively written as:

$$\mathbf{v}_k^{\mathcal{N}} = \sum_1^{\mathcal{N}_v} v_k^i \phi^i, \quad h_k^{\mathcal{N}} = \sum_1^{\mathcal{N}_h} h_k^i \phi^i, \quad \mathbf{u}_k^{\mathcal{N}} = \sum_1^{\mathcal{N}_u} u_k^i \psi^i, \quad \chi_k^{\mathcal{N}} = \sum_1^{\mathcal{N}_v} \chi_k^i \phi^i, \quad \text{and} \quad \lambda_k^{\mathcal{N}} = \sum_1^{\mathcal{N}_h} \lambda_k^i \phi^i. \quad (9)$$

Following the strategy presented in [28, 59, 60] for linear state equations and in [29] for Navier-Stokes equations, we define  $\bar{v} = [v_1, \dots, v_{N_t}]^T$ ,  $\bar{h} = [h_1, \dots, h_{N_t}]^T$  and  $\bar{u} = [u_1, \dots, u_{N_t}]^T$ , where  $v_k, h_k$  and  $u_k$  are the row vectors of the FE coefficients for state discrete variables at each time step. The vectors representing the initial condition for the velocity field  $\mathbf{v}$  and the water height  $h$  are  $\bar{v}_0 = [v_0, 0, \dots, 0]^T$  and  $\bar{h}_0 = [h_0, 0, \dots, 0]^T$ , respectively. Following the same argument, we can define both adjoint vectors  $\bar{\chi} = [\chi_1, \dots, \chi_{N_t}]^T$  and  $\bar{\lambda} = [\lambda_1, \dots, \lambda_{N_t}]^T$  and the desired profiles  $\bar{v}_d = [v_{d1}, \dots, v_{dN_t}]^T$  and  $\bar{h}_d = [h_{d1}, \dots, h_{dN_t}]^T$ . Also in this case,  $\chi_k$  and  $\lambda_k$  represent the vectors of the component of the FE variables at the  $k$ -th time step, for  $k = 1, \dots, N_t$ . Moreover, with  $\mathbf{w}^\mathcal{N} := (\mathbf{v}^\mathcal{N}, h^\mathcal{N}, \mathbf{u}^\mathcal{N}, \boldsymbol{\chi}^\mathcal{N}, \boldsymbol{\lambda}^\mathcal{N})$  we refer to the global FE variable including all the time instances, i.e. the  $\star^\mathcal{N}$  for  $\star = \mathbf{v}, h, \mathbf{u}, \boldsymbol{\chi}, \boldsymbol{\lambda}$  will indicate discretized space-time variables.

The shown structure is consistent with the space-time formulation exploited in several works as [67, 69, 70]: in this specific case, the backward Euler scheme in time coincides with a piecewise constants Discontinuous Galerkin approach as underlined in [22]. Although, for the sake of simplicity, we will always refer to Euler's schemes.

First of all, let us proceed with the discretization of the *state equation* governing the problem (1). Using a backward Euler, the *state equation* is discretized forward in time. The discretization gives the following result for the governing equation at each time step:

$$\begin{cases} \frac{\mathbf{v}_{k+1}^\mathcal{N} - \mathbf{v}_k^\mathcal{N}}{\Delta t} + \mu_1 \Delta \mathbf{v}_{k+1} + \mu_2 (\mathbf{v}_{k+1}^\mathcal{N} \cdot \nabla) \mathbf{v}_{k+1}^\mathcal{N} + g \nabla (h_{k+1}^\mathcal{N}) = \mathbf{u}_{k+1}^\mathcal{N} & \text{for } k \in \{0, \dots, N_t - 1\}, \\ \frac{h_{k+1}^\mathcal{N} - h_k^\mathcal{N}}{\Delta t} + \text{div}(h_{k+1}^\mathcal{N} \mathbf{v}_{k+1}^\mathcal{N}) = 0 & \text{for } k \in \{0, \dots, N_t - 1\}. \end{cases} \quad (10)$$

The same discretization strategy can be applied for the *optimality equation*. In this case, at each time step, one solves the equation:

$$\alpha \Delta t \mathbf{u}_k^\mathcal{N} = \Delta t \boldsymbol{\chi}_k^\mathcal{N} \quad \text{for } k \in \{1, \dots, N_t\}. \quad (11)$$

The last step of our full order discretization involves the *adjoint equation*. Since we are given the value of the adjoint variables at time  $T$ , the equations are discretized backward in time, through a forward Euler's method. In this case, at each time step, we have to solve the following system:

$$\begin{cases} \mathbf{v}_{k-1}^\mathcal{N} + \frac{\boldsymbol{\chi}_{k-1}^\mathcal{N} - \boldsymbol{\chi}_k^\mathcal{N}}{\Delta t} + \mu_1 \Delta \boldsymbol{\chi}_{k-1}^\mathcal{N} - \mu_2 (\mathbf{v}_{k-1}^\mathcal{N} \cdot \nabla) \boldsymbol{\chi}_{k-1}^\mathcal{N} \\ \quad + \mu_2 (\nabla \mathbf{v}_{k-1}^\mathcal{N})^T \boldsymbol{\chi}_{k-1}^\mathcal{N} - h_{k-1}^\mathcal{N} \nabla \lambda_{k-1}^\mathcal{N} = \mathbf{v}_{d_{k-1}}^\mathcal{N} & \text{for } k \in \{N_t, \dots, 2\}, \\ h_{k-1}^\mathcal{N} + \frac{\lambda_{k-1}^\mathcal{N} - \lambda_k^\mathcal{N}}{\Delta t} - \mathbf{v}_{k-1}^\mathcal{N} \cdot \nabla \lambda_{k-1}^\mathcal{N} - g \text{div}(\boldsymbol{\chi}_{k-1}^\mathcal{N}) = h_{d_{k-1}}^\mathcal{N} & \text{for } k \in \{N_t, \dots, 2\}. \end{cases} \quad (12)$$

We now have all the ingredients to define the whole discrete optimality system, i.e. given a  $\boldsymbol{\mu} \in \mathcal{P}$  find the vector  $\bar{w} = [[\bar{v}, \bar{h}], \bar{u}, [\bar{\chi}, \bar{\lambda}]]$  which solves the following nonlinear system

$$\mathcal{R}(\mathbf{w}^\mathcal{N}, \boldsymbol{\mu}) = \mathcal{G}(\mathbf{w}^\mathcal{N}; \boldsymbol{\mu}) \bar{w} - \bar{f} = 0, \quad (13)$$

where  $\mathcal{R}(\bar{w}, \boldsymbol{\mu})$  represents the residual vector given by the difference of the action of our nonlinear optimality equations and the right hand side vector, respectively denoted with  $\mathcal{G}(\mathbf{w}^\mathcal{N}, \boldsymbol{\mu})$  and  $\bar{f}$ . In order to find the space-time optimal solution  $\bar{w}$ , we rely on Newton's method, i.e., defining  $\mathbb{J}(\bar{w}; \boldsymbol{\mu}) = \mathbb{D}(\mathcal{G}(\mathbf{w}^\mathcal{N}; \boldsymbol{\mu}) \bar{w})$  the Frechét derivative of the operator  $\mathcal{G}(\mathbf{w}^\mathcal{N}; \boldsymbol{\mu}) \bar{w}$ , we iterate the solution

$$\bar{w}^{j+1} := \bar{w}^j + \mathbb{J}(\bar{w}^j; \boldsymbol{\mu})^{-1} (-\mathcal{R}(\mathbf{w}^{\mathcal{N}^j}; \boldsymbol{\mu})), \quad j \in \mathbb{N}, \quad (14)$$

until the convergence is reached.

We will now to focus on the algebraic structure presented just before. First of all, we specify the

nature of the residual vector  $\mathcal{R}(\mathbf{w}^N; \boldsymbol{\mu})$ . Then, we aim at underlying the saddle point structure of  $\mathbb{J}(\bar{\mathbf{w}}; \boldsymbol{\mu})$ . This concept is fundamental in order for our formulation to comply with classical references for optimization problems such as [11, 28, 29, 59, 60]. Moreover, the saddle point structure arising from linearization justifies the reduction techniques proposed in Section 3.3, already exploited for linear steady OCP( $\boldsymbol{\mu}$ )s in [46, 47, 54] and, for time dependent problems in [62, 63].

At this purpose, we define  $M_v$ ,  $M_u$  and  $M_h$  as mass matrices with respect to the variables  $\mathbf{v}$ ,  $\mathbf{u}$  and  $h$ , respectively, and  $K$ ,  $D$ ,  $H(\mathbf{v}_k^N)$ ,  $\bar{H}^*(\mathbf{v}_k^N)$ ,  $G(\mathbf{v}_k^N)$ ,  $G^*(\mathbf{v}_k^N)$  and  $F^*(h_k^N)$  where:

$$\begin{aligned} (K)_{ij} &= a_1((\phi_j, \phi_j), (\phi_i, \phi_i)), & (D)_{ij} &= a_2((\phi_j, \phi_j), (\phi_i, \phi_i)), \\ (H(\mathbf{v}_k^N))_{ij} &= a_1^{\text{nl}}((\mathbf{v}_k^N, h_k^N), (\phi_j, \phi_j), (\phi_i, \phi_i)), & (G(\mathbf{v}_k^N))_{ij} &= a_2^{\text{nl}}((\mathbf{v}_k^N, h_k^N), (\phi_j, \phi_j), (\phi_i, \phi_i)), \\ (\bar{H}^*(\mathbf{v}_k^N))_{ij} &= \int_{\Omega} (\nabla \mathbf{v}_k^N)^T \phi_i \phi_j d\Omega, & (G^*(\mathbf{v}_k^N))_{ij} &= a_3^{\text{nl}*}((\mathbf{v}_k^N, h_k^N), (\phi_i, \phi_i), (\phi_j, \phi_j)), \\ (F^*(h_k^N))_{ij} &= a_2^{\text{nl}*}((\mathbf{v}_k^N, h_k^N), (\phi_i, \phi_i), (\phi_j, \phi_j)). \end{aligned}$$

Moreover, for the sake of notation, let us define the operators  $S(\mathbf{v}_k^N) = \mu_1 \Delta t K + \mu_2 \Delta t H(\mathbf{v}_k^N)$  and  $S^*(\mathbf{v}_k^N) = \mu_1 \Delta t K - \mu_2 \Delta t H(\mathbf{v}_k^N) + \mu_2 \Delta t \bar{H}^*(\mathbf{v}_k^N)$ . Then, the explicit form for the residual vector is

$$\mathcal{R}(\mathbf{w}^N; \boldsymbol{\mu}) = \underbrace{\begin{bmatrix} \Delta t \mathcal{M}_v \bar{v} + \mathcal{K}_1^*(\mathbf{v}^N) \bar{\chi} + \mathcal{K}_2^*(h^N) \bar{\lambda} \\ \Delta t \mathcal{M}_h \bar{h} + \mathcal{K}_3^* \bar{\chi} + \mathcal{K}_4^*(\mathbf{v}^N) \bar{\lambda} \\ \alpha \Delta t \mathcal{M}_u \bar{u} - \Delta t \mathcal{M}_u \bar{\chi} \\ \mathcal{K}_1(\mathbf{v}^N) \bar{v} + \mathcal{K}_2 \bar{h} - \Delta t \mathcal{M}_u \bar{u} \\ \mathcal{K}_4(\mathbf{v}^N) \bar{h} \end{bmatrix}}_{\mathcal{G}(\bar{\mathbf{w}}; \boldsymbol{\mu}) \bar{\mathbf{w}}} - \underbrace{\begin{bmatrix} \Delta t \mathcal{M}_v \bar{v}_d \\ \Delta t \mathcal{M}_h \bar{h}_d \\ \bar{0} \\ \mathcal{M}_v \bar{v}_0 \\ \mathcal{M}_h \bar{h}_0 \end{bmatrix}}_{\bar{\mathbf{f}}}, \quad (15)$$

where  $\mathcal{M}_v$ ,  $\mathcal{M}_h$  and  $\mathcal{M}_u$  are block diagonal matrices with diagonal entries  $\{M_v, \dots, M_v\}$ ,  $\{M_h, \dots, M_h\}$  and  $\{M_u, \dots, M_u\}$ , respectively. Moreover we define the block diagonal matrices given by  $\mathcal{K}_2 = \text{diag}\{\Delta t D, \dots, \Delta t D\}$ ,  $\mathcal{K}_2^*(h^N) = \text{diag}\{\Delta t F^*(h_1^N), \dots, \Delta t F^*(h_{N_t}^N)\}$ ,  $\mathcal{K}_3^* = \text{diag}\{\Delta t D^T, \dots, \Delta t D^T\}$  and the matrices

$$\begin{aligned} \mathcal{K}_1(\mathbf{v}^N) &= \begin{bmatrix} M_v + S(\mathbf{v}_1^N) & 0 & \dots & \dots & 0 \\ -M_v & M_v + S(\mathbf{v}_2^N) & 0 & \dots & 0 \\ 0 & -M_v & M_v + S(\mathbf{v}_3^N) & 0 & \dots & 0 \\ & & \ddots & \ddots & \\ 0 & \dots & & 0 & -M_v & M_v + S(\mathbf{v}_{N_t}^N) \end{bmatrix}, \\ \mathcal{K}_4(\mathbf{v}^N) &= \begin{bmatrix} M_h + \Delta t G(\mathbf{v}_1^N) & 0 & \dots & \dots & 0 \\ -M_h & M_h + \Delta t G(\mathbf{v}_2^N) & 0 & \dots & 0 \\ 0 & -M_h & M_h + \Delta t G(\mathbf{v}_3^N) & 0 & \dots & 0 \\ & & \ddots & \ddots & \\ 0 & \dots & & 0 & -M_h & M_h + \Delta t G(\mathbf{v}_{N_t}^N) \end{bmatrix}, \\ \mathcal{K}_1^*(\mathbf{v}^N) &= \begin{bmatrix} M_v + S^*(\mathbf{v}_1^N) & -M_v & \dots & \dots & 0 \\ 0 & M_v + S^*(\mathbf{v}_2^N) & -M_v & \dots & 0 \\ & & \ddots & \ddots & \\ 0 & \dots & 0 & M_v + S^*(\mathbf{v}_{N_t-1}^N) & -M_v & 0 \\ 0 & \dots & & & 0 & M_v + S^*(\mathbf{v}_{N_t}^N) \end{bmatrix}, \end{aligned}$$

$$\text{and } \mathcal{K}_4^*(\mathbf{v}^\mathcal{N}) = \begin{bmatrix} M_h + G^*(\mathbf{v}_1^\mathcal{N}) & -M_h & \cdots & & & 0 \\ 0 & M_h + G^*(\mathbf{v}_2^\mathcal{N}) & -M_h & & \cdots & 0 \\ & & \ddots & & \ddots & \\ 0 & \cdots & 0 & M_h + G^*(\mathbf{v}_{N_t-1}^\mathcal{N}) & -M_h & 0 \\ 0 & \cdots & & & 0 & M_h + G^*(\mathbf{v}_{N_t}^\mathcal{N}) \end{bmatrix}.$$

The residual  $\mathcal{R}(\mathbf{w}^\mathcal{N}; \boldsymbol{\mu})$  can be also written in the following compact form

$$\mathcal{R}(\mathbf{w}^\mathcal{N}; \boldsymbol{\mu}) = \begin{bmatrix} \Delta t \mathcal{M}[\bar{v}, \bar{h}] + \mathcal{K}^*(\mathbf{v}^\mathcal{N}, h^\mathcal{N})[\bar{\chi}, \bar{\lambda}] \\ \alpha \Delta t \mathcal{M}_u \bar{u} - \Delta t \mathcal{M}_u \bar{\chi} \\ \mathcal{K}(\mathbf{v}^\mathcal{N})[\bar{v}, \bar{h}] - \Delta t \mathcal{M}_{u0}[\bar{u}, \bar{0}] \end{bmatrix} - \begin{bmatrix} \Delta t \mathcal{M}[\bar{v}_d, \bar{h}_d] \\ \bar{0} \\ \mathcal{M}[\bar{v}_0, \bar{h}_0] \end{bmatrix}, \quad (16)$$

where  $\mathcal{M} = \begin{bmatrix} \mathcal{M}_v & 0 \\ 0 & \mathcal{M}_h \end{bmatrix}$ ,  $\mathcal{K}(\mathbf{v}^\mathcal{N}) = \begin{bmatrix} \mathcal{K}_1(\mathbf{v}^\mathcal{N}) & \mathcal{K}_2 \\ 0 & \mathcal{K}_4(\mathbf{v}^\mathcal{N}) \end{bmatrix}$ ,  $\mathcal{K}^*(\mathbf{v}^\mathcal{N}, h^\mathcal{N}) = \begin{bmatrix} \mathcal{K}_1^*(\mathbf{v}^\mathcal{N}) & \mathcal{K}_2^*(h^\mathcal{N}) \\ \mathcal{K}_3^* & \mathcal{K}_4^*(\mathbf{v}^\mathcal{N}) \end{bmatrix}$  and  $\mathcal{M}_{u0} = \begin{bmatrix} \mathcal{M}_u & 0 \\ 0 & 0 \end{bmatrix}$ . We remark that the first, the second and the last row of  $\mathcal{R}(\mathbf{w}^\mathcal{N}, \boldsymbol{\mu})$  represent adjoint, optimality and state equations, respectively.

We want now focus our attention on  $\mathbb{J}(\bar{w}; \boldsymbol{\mu})$ . Indeed, we aim at underlying the saddle point structure of  $\mathbb{J}(\bar{w}; \boldsymbol{\mu})$ . This concept is fundamental in order for our formulation to comply with classical references for optimization problems such as [11, 28, 29, 59, 60]. Moreover, the saddle point structure arising from linearization, justifies the reduction techniques proposed in Section 3.3, already exploited for linear steady OCP( $\boldsymbol{\mu}$ )s in [46, 47, 54] and, for time dependent problems in [62, 63]. For the sake of clarification, we underline that with the notation  $(\cdot)^\mathbb{D}$ , we denote a quantity which *derives* from the differentiation of operators. The differentiation will be applied to general space-time variables that are denoted with  $[v, h], u, [\chi, \lambda]$ , for state, control and adjoint space, respectively.

Let us start our analysis with the state equation. New operators are needed:  $\bar{H}(\mathbf{v}_k^\mathcal{N})$ , with  $\bar{H}(\mathbf{v}_k^\mathcal{N})_{ij} = a_1^{\text{nl}}((\phi_j, \phi_j), (\mathbf{v}_k^\mathcal{N}, h_k^\mathcal{N}), (\phi_i, \phi_i))$ , and  $F(h_k^\mathcal{N})$  with  $F(h_k^\mathcal{N})_{ij} = a_2^{\text{nl}}((\phi_j, \phi_j), (\mathbf{v}_k^\mathcal{N}, h_k^\mathcal{N}), (\phi_i, \phi_i))$ . Then, defining  $S(\mathbf{v}_k^\mathcal{N})^\mathbb{D} := \mathbb{D}(S(\mathbf{v}_k^\mathcal{N})v_k) = \mu_1 \Delta t K + \mu_2 \Delta t H(\mathbf{v}_k^\mathcal{N}) + \mu_2 \Delta t \bar{H}(\mathbf{v}_k^\mathcal{N})$ , we can differentiate the state equation as follows:  $\mathbb{D}(\mathcal{K}(\mathbf{v}^\mathcal{N})[\bar{v}, \bar{h}] - \Delta t \mathcal{M}_u \bar{u})$ . The process will affect only nonlinear terms and will lead to a linearized system of the form

$$\mathcal{K}^\mathbb{D}(\mathbf{v}^\mathcal{N}, h^\mathcal{N})[v, h] - \Delta t \mathcal{M}_u u, \quad (17)$$

with  $\mathcal{K}^\mathbb{D} = \begin{bmatrix} \mathcal{K}_1^\mathbb{D}(\mathbf{v}^\mathcal{N}) & \mathcal{K}_2 \\ \mathcal{K}_3^\mathbb{D}(h^\mathcal{N}) & \mathcal{K}_4(\mathbf{v}^\mathcal{N}) \end{bmatrix}$  where  $\mathcal{K}_3^\mathbb{D} = \text{diag}\{F(h_1^\mathcal{N}), \dots, F(h_{N_t}^\mathcal{N})\}$ ,

$$\mathcal{K}_1^\mathbb{D} = \begin{bmatrix} M_v + S(\mathbf{v}_1^\mathcal{N})^\mathbb{D} & 0 & \cdots & & & 0 \\ -M_v & M_v + S(\mathbf{v}_2^\mathcal{N})^\mathbb{D} & 0 & \cdots & & 0 \\ 0 & -M_v & M_v + S(\mathbf{v}_3^\mathcal{N})^\mathbb{D} & 0 & \cdots & 0 \\ & & \ddots & \ddots & & \\ 0 & \cdots & & 0 & -M_v & M_v + S(\mathbf{v}_{N_t}^\mathcal{N})^\mathbb{D} \end{bmatrix}.$$

The differentiation of the optimality equation (11) leads to the same equation, due to its linearity. Let us differentiate the *adjoint equation*. In order to write the linearized system we define four more operators:  $H^*(\chi_k^\mathcal{N})$ ,  $\bar{H}^*(\chi_k^\mathcal{N})$ ,  $\bar{F}(\lambda_k^\mathcal{N})$  and  $\bar{G}(\lambda_k^\mathcal{N})$  where:

$$(H^*(\chi_k^\mathcal{N}))_{ij} = - \int_{\Omega} (\phi_i \cdot \nabla) \chi_k^\mathcal{N} \phi_j \, d\Omega, \quad (\bar{H}^*(\chi_k^\mathcal{N}))_{ij} = \int_{\Omega} (\nabla \phi_i^\mathcal{N})^T \chi_k^\mathcal{N} \phi_j \, d\Omega,$$

$$(\bar{F}(\lambda_k^\mathcal{N}))_{ij} = a_2^{\text{nl}}((\phi_j, \phi_j), (\chi_k^\mathcal{N}, \lambda_k^\mathcal{N}), (\phi_j, \phi_j)) \text{ and } (\bar{G}(\lambda_k^\mathcal{N}))_{ij} = a_2^{\text{nl}}((\phi_j, \phi_j), (\chi_k^\mathcal{N}, \lambda_k^\mathcal{N}), (\phi_j, \phi_j)).$$

Thanks to these quantities, we can perform the differentiation of the adjoint equation

$$\mathbb{D}(\Delta t \mathcal{M}[\bar{v}, \bar{h}] + \mathcal{K}^*(\mathbf{v}^\mathcal{N}, h^\mathcal{N})[\bar{\chi}, \bar{\lambda}]),$$

which will result in the following linearized system

$$\Delta t \underbrace{(\mathcal{M} + \mathcal{K}^{*\mathbb{D}}(\boldsymbol{\chi}^\mathcal{N}, \lambda^\mathcal{N}))}_{\mathcal{M}^\mathbb{D}(\boldsymbol{\chi}^\mathcal{N}, \lambda^\mathcal{N})}[\underline{v}, \underline{h}] + \mathcal{K}^*(\mathbf{v}^\mathcal{N}, h^\mathcal{N})[\underline{\chi}, \underline{\lambda}], \quad (18)$$

where  $\mathcal{M}^\mathbb{D} = \begin{bmatrix} \mathcal{M}_1^\mathbb{D}(\boldsymbol{\chi}^\mathcal{N}) & \mathcal{M}_2^\mathbb{D}(\lambda^\mathcal{N}) \\ \mathcal{M}_3^\mathbb{D}(\lambda^\mathcal{N}) & \mathcal{M}_4^\mathbb{D} \end{bmatrix}$  with the block diagonal matrices defined by

$\mathcal{M}_1^\mathbb{D}(\boldsymbol{\chi}^\mathcal{N}) = \text{diag}\{M_v + \mu_2 H^*(\chi_1^\mathcal{N}) + \mu_2 \bar{H}^*(\chi_1^\mathcal{N}), \dots, M_v + \mu_2 H^*(\chi_{N_t}^\mathcal{N}) + \mu_2 \bar{H}^*(\chi_{N_t}^\mathcal{N})\}$ ,  
 $\mathcal{M}_2^\mathbb{D}(\lambda^\mathcal{N}) = \text{diag}\{\bar{F}(\lambda_1^\mathcal{N}), \dots, \bar{F}(\lambda_{N_t}^\mathcal{N})\}$ ,  $\mathcal{M}_3^\mathbb{D}(\lambda^\mathcal{N}) = \text{diag}\{\bar{G}(\lambda_1^\mathcal{N}), \dots, \bar{G}(\lambda_{N_t}^\mathcal{N})\}$  and  
 $\mathcal{M}_4^\mathbb{D} = \text{diag}\{M_h, \dots, M_h\}$ . We underline that, in (16) the  $\mathcal{K}^* \neq \mathcal{K}^T$ , due to the nonlinearity of the involved forms in the system, then no saddle point structure arises. However, we can recast the linearized problem in a saddle point formulation since  $\mathcal{K}^* \equiv \mathcal{K}^{\mathbb{D}T}$ . Indeed, calling with  $\bar{x}$  the state-control space-time vector variable  $[[\bar{v}, \bar{h}], \bar{u}]$  and with  $\bar{p} = [\bar{\chi}, \bar{\lambda}]$  the adjoint variable, and defining

$$\mathbf{A} = \begin{bmatrix} \Delta t \mathcal{M}^\mathbb{D} & 0 \\ 0 & \alpha \Delta t \mathcal{M}_u \end{bmatrix} \quad \text{and} \quad \mathbf{B} = \begin{bmatrix} \mathcal{K}^\mathbb{D} & -\Delta t \mathcal{M}_u \end{bmatrix},$$

it is simple to remark that the Frechét derivative can be read in the following saddle point framework:

$$\mathbb{J}(\bar{w}; \boldsymbol{\mu}) \bar{w} = \begin{bmatrix} \mathbf{A} & \mathbf{B}^T \\ \mathbf{B} & 0 \end{bmatrix} \begin{bmatrix} \bar{x} \\ \bar{p} \end{bmatrix}. \quad (19)$$

Given a parameter  $\boldsymbol{\mu} \in \mathcal{P}$ , we derive the truth optimal solution from a direct solution of the system (16), dealing with the saddle point structure presented in (19) at each iteration of Newton's solver. We remark that  $\mathbb{J}(\bar{w}; \boldsymbol{\mu})$  is actually a generalized saddle point matrix, see [11] as references, where  $\mathbf{A} \neq \mathbf{A}^T$ . Still, we will always talk about saddle point structure from now on, since the generalization does not affect the reduced strategy used [14]: indeed, the solvability condition remains the fulfillment of the inf-sup condition [6, 13, 15] over the state equation for the symmetric part of  $\mathbf{A}$ . Moreover, the saddle point structure does not depend on the discretization scheme used: it can be generalized for other space and time approximations. As already specified in Section 1, in a parametric context, FE solutions could be unfeasible due to the huge computational effort required, most of all in time dependent setting, where the system to be solved has  $\mathcal{N}_{\text{tot}} = N_t \times \mathcal{N}$  as actual dimension. In the next Section, we will describe reduced order modelling (ROM) techniques, that we use in order to overcome the problem of finding the parametric solution of an expensive optimal control system.

### 3 ROM Approximation for OCP( $\boldsymbol{\mu}$ )s

In this Section, we recall a brief introduction on ROM approximation techniques and we show how to exploit it in the solution of SWEs optimal control parametrized systems. Even if we propose the reduced strategy for a very specific governing state equation the approach could be used for general problems: indeed, we refer to [41, 61, 71] for previous applications to nonlinear OCP( $\boldsymbol{\mu}$ )s. Besides, in order to deal with time dependency, we follow the numerical strategy already presented in [62, 63]. We start with general basics and ideas which guarantee an efficient ROM applicability and then, in Section 3.2, we will move towards the Proper Orthogonal Decomposition (POD) algorithm, see for example [9, 16, 19, 27] as references. In the end, we will extend the aggregated space strategy to our problem, as an adaptation of what is already known for linear OCP( $\boldsymbol{\mu}$ )s in [20, 47, 46].

### 3.1 Reduced Problem Formulation

In Section 2.1, we proposed optimal flow control as a way to formulate inverse problems in marine environmental sciences, exploiting the velocity-height model of SWE. As we already specified in Section 1, the FE method could be computationally unfeasible when interested in solving several instances of the proposed  $\text{OCP}(\boldsymbol{\mu})$ , most of all, in a parametrized setting. ROM techniques replace the FE *truth* system, with a surrogate one, which is often smaller in terms of dimension.

We now briefly introduce ROM ideas in the  $\text{OCP}(\boldsymbol{\mu})$ s setting. In order to clarify the role of the parametric setting, we will explicit the  $\boldsymbol{\mu}$ -dependency in the quantities involved in the reduction process.

By varying the value of  $\boldsymbol{\mu}$  in the parameter space  $\mathcal{P}$  the parametric solution of (5) will define a manifold

$$\mathcal{M} = \{(\mathbf{v}(\boldsymbol{\mu}), h(\boldsymbol{\mu}), \mathbf{u}(\boldsymbol{\mu}), \boldsymbol{\chi}(\boldsymbol{\mu}), \lambda(\boldsymbol{\mu})) \mid \boldsymbol{\mu} \in \mathcal{P}\}$$

which we assume to be smooth. If we restrict our attention to the FE approximation, the ensemble of the *truth* solutions is an approximation of  $\mathcal{M}$ :

$$\mathcal{M}^{\mathcal{N}_{\text{tot}}} = \{(\mathbf{v}^{\mathcal{N}}(\boldsymbol{\mu}), h^{\mathcal{N}}(\boldsymbol{\mu}), \mathbf{u}^{\mathcal{N}}(\boldsymbol{\mu}), \boldsymbol{\chi}^{\mathcal{N}}(\boldsymbol{\mu}), \lambda^{\mathcal{N}}(\boldsymbol{\mu})) \mid \boldsymbol{\mu} \in \mathcal{P}\}.$$

Also in this case, the variables  $\star^{\mathcal{N}}$  are actually considered in the space-time function spaces of dimension  $N_t \mathcal{N}_{\star}$  for  $\star = \mathbf{v}, h, \mathbf{u}, \boldsymbol{\chi}, \lambda$ , with  $\mathcal{N}_{\mathbf{v}} = \mathcal{N}_{\boldsymbol{\chi}}$  and  $\mathcal{N}_h = \mathcal{N}_{\lambda}$ , since the same discretized space is used for state and adjoint variables. ROM aims at describing the structure of the approximated solution manifold  $\mathcal{M}^{\mathcal{N}_{\text{tot}}}$  through the construction of basis derived from *snapshots*, i.e. properly chosen FE solutions of the variables involved in the optimization system. In other words, reduced spaces are subspaces of the FE spaces and they are chosen through algorithms that guarantee a proper description of how the optimality system (5) changes with respect to a new value of  $\boldsymbol{\mu}$ . After the basis function building process, a standard Galerkin projection is performed, in order to find a low-dimensional surrogate solution, which is computationally efficient and still accurate with respect to the FE model.

Let us assume to have already built the reduced function spaces  $\mathcal{Y}_N \subset \mathcal{Y}^{\mathcal{N}} \subset \mathcal{Y}$  and  $\mathcal{U}_N \subset \mathcal{U}^{\mathcal{N}} \subset \mathcal{U}$  for state/adjoint variables and control, respectively. The projected reduced  $\text{OCP}(\boldsymbol{\mu})$  reads: given  $\boldsymbol{\mu} \in \mathcal{P}$ , find  $((\mathbf{v}_N(\boldsymbol{\mu}), h_N(\boldsymbol{\mu})), \mathbf{u}_N(\boldsymbol{\mu}), (\boldsymbol{\chi}_N(\boldsymbol{\mu}), \lambda_N(\boldsymbol{\mu})))$  which solves:

$$\begin{cases} D_{\mathbf{v}} \mathcal{L}((\mathbf{v}_N(\boldsymbol{\mu}), h_N(\boldsymbol{\mu})), \mathbf{u}_N(\boldsymbol{\mu}), (\boldsymbol{\chi}_N(\boldsymbol{\mu}), \lambda_N(\boldsymbol{\mu})))[\mathbf{z}] = 0 & \forall \mathbf{z} \in \mathcal{Y}_{\mathbf{v}N}, \\ D_h \mathcal{L}((\mathbf{v}_N(\boldsymbol{\mu}), h_N(\boldsymbol{\mu})), \mathbf{u}_N(\boldsymbol{\mu}), (\boldsymbol{\chi}_N(\boldsymbol{\mu}), \lambda_N(\boldsymbol{\mu})))[q] = 0 & \forall q \in \mathcal{Y}_{hN}, \\ D_{\mathbf{u}} \mathcal{L}((\mathbf{v}_N(\boldsymbol{\mu}), h_N(\boldsymbol{\mu})), \mathbf{u}_N(\boldsymbol{\mu}), (\boldsymbol{\chi}_N(\boldsymbol{\mu}), \lambda_N(\boldsymbol{\mu})))[\boldsymbol{\tau}] = 0 & \forall \boldsymbol{\tau} \in \mathcal{U}_N, \\ D_{\boldsymbol{\chi}} \mathcal{L}((\mathbf{v}_N(\boldsymbol{\mu}), h_N(\boldsymbol{\mu})), \mathbf{u}_N(\boldsymbol{\mu}), (\boldsymbol{\chi}_N(\boldsymbol{\mu}), \lambda_N(\boldsymbol{\mu})))[\boldsymbol{\kappa}] = 0 & \forall \boldsymbol{\kappa} \in \mathcal{Y}_{\boldsymbol{\chi}N}, \\ D_{\lambda} \mathcal{L}((\mathbf{v}_N(\boldsymbol{\mu}), h_N(\boldsymbol{\mu})), \mathbf{u}_N(\boldsymbol{\mu}), (\boldsymbol{\chi}_N(\boldsymbol{\mu}), \lambda_N(\boldsymbol{\mu})))[\xi] = 0 & \forall \xi \in \mathcal{Y}_{\lambda N}. \end{cases} \quad (20)$$

The reduced system (20) is still nonlinear and it can be solved thanks to a Newton method, as already specified in Section 2.3. In the next sections, we will show an approach that leads to the construction of reduced spaces and what are the techniques to be used in order to deal with the reduced Frechét derivative aiming at preserving the saddle point structure shown in (19) and its stability.

### 3.2 POD Algorithm for $\text{OCP}(\boldsymbol{\mu})$ s

In order to build a reduced environment, two of the major techniques that have been exploited in the literature are POD [9, 16, 19, 27] and greedy algorithm [25, 27, 46, 47, 55]. We decided to rely on the first approach since the applicability of the latter requires an error estimator, which



is still not available for our nonlinear time dependent optimization problem.

We now describe the POD algorithm which consists in two phases: an exploratory process based on a sample in the parameter space, in order to generate  $N_{\max}$  snapshots and a compressing stage, where the snapshots are manipulated and  $N < N_{\max}$  basis functions are generated with the elimination of redundant information. We provide the algorithm description as proposed in [9, 16, 19, 27]. First of all, a discrete subset of parameters  $\mathcal{P}_{N_{\max}} \subset \mathcal{P}$  is chosen. If we compute FE solutions for  $\boldsymbol{\mu} \in \mathcal{P}_{N_{\max}}$  we obtain the following sampled manifold:

$$\mathcal{M}_h^{\mathcal{N}_{\text{tot}}} = \{(\mathbf{v}^{\mathcal{N}}(\boldsymbol{\mu}), h^{\mathcal{N}}(\boldsymbol{\mu}), \mathbf{u}^{\mathcal{N}}(\boldsymbol{\mu}), \boldsymbol{\chi}^{\mathcal{N}}(\boldsymbol{\mu}), \lambda^{\mathcal{N}}(\boldsymbol{\mu})) \mid \boldsymbol{\mu} \in \mathcal{P}_{N_{\max}}\} \subset \mathcal{M}^{\mathcal{N}_{\text{tot}}}.$$

We define  $N_{\max}$  as the cardinality of the set  $\mathcal{P}_{N_{\max}}$  and it is clear that, when  $N_{\max}$  is large enough, the sampled manifold  $\mathcal{M}_h^{\mathcal{N}_{\text{tot}}}$  is a reliable surrogate of  $\mathcal{M}^{\mathcal{N}_{\text{tot}}}$ .

We decided to apply the POD algorithm separately for all the variables involved in the system: we refer to this strategy as *partitioned approach*. The final goal of the POD is to provide reduced spaces of dimension  $N$  which realize the minimum of the quantities:

$$\begin{aligned} & \sqrt{\frac{1}{N_{\max}} \sum_{\boldsymbol{\mu} \in \mathcal{P}_{N_{\max}}} \min_{z_N \in \mathcal{Y}_v} \|\mathbf{v}^{\mathcal{N}}(\boldsymbol{\mu}) - z_N\|_{\mathcal{Y}_v}^2}, \quad \sqrt{\frac{1}{N_{\max}} \sum_{\boldsymbol{\mu} \in \mathcal{P}_{N_{\max}}} \min_{q_N \in \mathcal{Y}_h} \|h^{\mathcal{N}}(\boldsymbol{\mu}) - q_N\|_{\mathcal{Y}_h}}, \\ & \sqrt{\frac{1}{N_{\max}} \sum_{\boldsymbol{\mu} \in \mathcal{P}_{N_{\max}}} \min_{\boldsymbol{\tau}_N \in \mathcal{U}_N} \|\mathbf{u}^{\mathcal{N}}(\boldsymbol{\mu}) - \boldsymbol{\tau}_N\|_{\mathcal{U}}^2}, \\ & \sqrt{\frac{1}{N_{\max}} \sum_{\boldsymbol{\mu} \in \mathcal{P}_{N_{\max}}} \min_{\boldsymbol{\kappa}_N \in \mathcal{Y}_v} \|\boldsymbol{\chi}^{\mathcal{N}}(\boldsymbol{\mu}) - \boldsymbol{\kappa}_N\|_{\mathcal{Y}_v}^2}, \quad \sqrt{\frac{1}{N_{\max}} \sum_{\boldsymbol{\mu} \in \mathcal{P}_{N_{\max}}} \min_{\xi_N \in \mathcal{Y}_h} \|\lambda^{\mathcal{N}}(\boldsymbol{\mu}) - \xi_N\|_{\mathcal{Y}_h}}. \end{aligned}$$

We now summarise the POD-Galerkin procedure algorithm only for the velocity variable  $\mathbf{v}(\boldsymbol{\mu})$ . In any case, the proposed approach can be identically used for the other four variables as well. Let us define a set of ordered parameters  $\boldsymbol{\mu}_1, \dots, \boldsymbol{\mu}_{N_{\max}} \in \mathcal{P}_{N_{\max}}$ . To this parametric set, it will correspond an ordered ensemble of FE solutions, i.e. snapshots,  $\mathbf{v}^{\mathcal{N}}(\boldsymbol{\mu}_1), \dots, \mathbf{v}^{\mathcal{N}}(\boldsymbol{\mu}_{N_{\max}})$ . We can now define the correlation matrix  $\mathbf{C}^v \in \mathbb{R}^{N_{\max} \times N_{\max}}$  of snapshots of the velocity state variable, i.e.:

$$\mathbf{C}_{ml}^v = \frac{1}{N_{\max}} (\mathbf{v}^{\mathcal{N}}(\boldsymbol{\mu}_m), \mathbf{v}^{\mathcal{N}}(\boldsymbol{\mu}_l))_{\mathcal{Y}}, \quad 1 \leq m, l \leq N_{\max}.$$

The next step is to solve the following eigenvalue problem

$$\mathbf{C}^v \mathbf{x}_n^v = \theta_n^v \mathbf{x}_n^v, \quad 1 \leq n \leq N,$$

with  $\|\mathbf{x}_n^v\|_{\mathcal{Y}} = 1$ . Assuming that the eigenvalues  $\theta_1^v, \dots, \theta_{N_{\max}}^v$  are sorted in decreasing order we retain only the first  $N$  ones, namely  $\theta_1^v, \dots, \theta_N^v$ , and the corresponding eigenvectors  $\mathbf{x}_1^v, \dots, \mathbf{x}_N^v$ . We can now build ordered basis functions  $\{\zeta_1^v, \dots, \zeta_N^v\}$  spanning the reduced space  $\mathcal{Y}_{vN}$ . Defining  $(x_n^v)_m$  as the  $m$ -th component of the state velocity eigenvector  $\mathbf{x}_n^v \in \mathbb{R}^M$ , the basis functions are given by the following relation:

$$\zeta_n^v = \frac{1}{\sqrt{\theta_n^v}} \sum_{m=1}^M (x_n^v)_m \mathbf{v}^{\mathcal{N}}(\boldsymbol{\mu}_m), \quad 1 \leq n \leq N.$$

Even if we performed a different POD algorithm for all the involved variables, we have not separate time instances: indeed, the snapshots are FE solutions including all the considered temporal steps. This strategy is consistent with respect to the space-time FE full order discretization introduced in Section 2.3. Moreover, the final reduced model preserves the space-time structure. In the next Section we analyze how the obtained basis functions, i.e.  $\{\zeta_n^v\}_{n=1}^N, \{\zeta_n^h\}_{n=1}^N, \{\zeta_n^u\}_{n=1}^N, \{\zeta_n^{\boldsymbol{\chi}}\}_{n=1}^N$  and  $\{\zeta_n^{\lambda}\}_{n=1}^N$  have to be manipulated in order to guarantee the solvability of system (16).

### 3.3 Aggregated Spaces Approach

It is very well known in the literature that optimization linear PDEs constraints leads to the the solution of system in saddle point formulation [11, 12, 30, 60]. The saddle point framework can be extended also for time dependent problems [28, 29, 59, 60]. The main point of solving problems based on the structure proposed in (19) is to guarantee the inf-sup condition for the matrix  $\mathbf{B}$ , which represents the state equation. In other words, for every  $\boldsymbol{\mu}$ , we want to verify the following inequality:

$$\inf_{0 \neq \bar{p}} \sup_{0 \neq \bar{x}} \frac{\bar{p}^T \mathbf{B} \bar{x}}{\|\bar{x}\|_{\mathcal{X}} \|\bar{p}\|_{\mathcal{Y}}} \geq \beta^{\mathcal{N}}(\boldsymbol{\mu}) > 0, \quad (21)$$

see [6, 13, 15] as references. At the FE level, relation (21) actually holds thanks to the hypothesis on the coincidence between state and adjoint FE discretized spaces, which is guaranteed by the same assumption at the continuous level, as we introduced in Section 2.2. Now, let us suppose to have applied standard POD described in Section 3.2 and have obtained the following basis matrices:

$$Z_{\bar{x}} = \begin{bmatrix} Z_v \\ Z_h \\ Z_u \end{bmatrix}, \quad Z_{\bar{p}} = \begin{bmatrix} Z_{\chi} \\ Z_{\lambda} \end{bmatrix} \quad \text{and} \quad Z = \begin{bmatrix} Z_{\bar{x}} \\ Z_{\bar{p}} \end{bmatrix},$$

where  $Z_{\star} = [\zeta_1^{\star} | \dots | \zeta_N^{\star}] \in \mathbb{R}^{N_t N_{\star} \times N}$ , for  $\star = v, h, u, \chi, \lambda$ . In order to solve the optimality system in an algebraic low dimensional framework a Galerkin projection is performed into the reduced spaces: indeed, this leads to a reduced system of the form

$$\mathcal{G}_N(\bar{w}_N; \boldsymbol{\mu}) \bar{w}_N = \bar{f}_N, \quad (22)$$

where

$$\mathcal{G}_N(\bar{w}_N; \boldsymbol{\mu}) := Z^T \mathcal{G}(Z \bar{w}_N; \boldsymbol{\mu}), \quad \bar{w}_N := Z^T \bar{w}, \quad \text{and} \quad \bar{f}_N := Z^T \bar{f}.$$

The system (22) is nonlinear, in order to solve it, we applied Newton's method and we iteratively

$$\bar{w}_N^{j+1} := \bar{w}_N^j + \mathbb{J}_N(\bar{w}_N^j; \boldsymbol{\mu})^{-1} (\bar{f}_N - \mathcal{G}(\bar{w}_N^j; \boldsymbol{\mu})), \quad j \in \mathbb{N}, \quad (23)$$

where the Frechét derivative preserves the saddle point structure, i.e.

$$\mathbb{J}_N(\bar{w}_N; \boldsymbol{\mu}) \bar{w}_N = \begin{bmatrix} \mathbf{A}_N & \mathbf{B}_N^T \\ \mathbf{B}_N & 0 \end{bmatrix} \begin{bmatrix} \bar{x}_N \\ \bar{p}_N \end{bmatrix}, \quad (24)$$

with  $J_N(\bar{w}_N; \boldsymbol{\mu}) = Z^T \mathbb{J}(Z \bar{w}_N; \boldsymbol{\mu}) Z$ ,  $\mathbf{A}_N = Z_{\bar{x}}^T \mathbf{A} Z_{\bar{x}}$ ,  $\mathbf{B}_N = Z_{\bar{p}}^T \mathbf{B} Z_{\bar{x}}$ ,  $\bar{x}_N := Z_{\bar{x}}^T \bar{x}$  and  $\bar{p}_N := Z_{\bar{p}}^T \bar{p}$ . Also at the reduced level, equation (24) implies that we still need to verify a *reduced inf-sup condition* of the form

$$\inf_{0 \neq \bar{p}_N} \sup_{0 \neq \bar{x}_N} \frac{\bar{p}_N^T \mathbf{B}_N \bar{x}_N}{\|\bar{x}_N\|_{\mathcal{X}} \|\bar{p}_N\|_{\mathcal{Y}}} \geq \beta_N(\boldsymbol{\mu}) > 0, \quad (25)$$

due to system (24). Once again, the inequality is verified if the reduced space for state and adjoint variables is the same. However, the POD procedure we introduced will not necessarily result in the same reduced order approximation for state and adjoint. Indeed, the application of the strategy described in Section 3.2 will lead to the following spaces:

$$\begin{aligned} \mathcal{Y}_{vN} &= \text{span}\{\zeta_n^v, n = 1, \dots, N\}, \\ \mathcal{Y}_{hN} &= \text{span}\{\zeta_n^h, n = 1, \dots, N\}, \\ \mathcal{Y}_{uN} &= \text{span}\{\zeta_n^u, n = 1, \dots, N\}, \\ \mathcal{Y}_{\chi N} &= \text{span}\{\zeta_n^{\chi}, n = 1, \dots, N\}, \\ \mathcal{Y}_{\lambda N} &= \text{span}\{\zeta_n^{\lambda}, n = 1, \dots, N\}. \end{aligned}$$

Let  $\mathcal{Q}_N$  be the product space of  $\mathcal{Y}_{\chi_N}$  and  $\mathcal{Y}_{\lambda_N}$ : in other words, the POD defines an adjoint space  $\mathcal{Q}_N \neq \mathcal{Y}_N$ , even if the state and the adjoint space are assumed to be the same at the continuous level. It is clear that, as already specified for the continuous and FE discretized system, in order to guarantee the solvability of the reduced optimality system, we have to build our reduced spaces in such a way the basis functions can describe state variables as well as adjoint variables. This goal is reached thanks to the aggregated spaces technique as presented in [20, 46, 47]. The main purpose of this strategy is to build a space that can be used both for state and adjoint variables. Then, let us define the aggregated spaces

$$\mathcal{Z}_{\mathbf{v}}^{\chi} = \text{span} \{ \zeta_n^{\mathbf{v}}, \zeta_n^{\chi}, n = 1, \dots, N \} \text{ and } \mathcal{Z}_{\mathbf{h}}^{\lambda} = \text{span} \{ \zeta_n^{\mathbf{h}}, \zeta_n^{\lambda}, n = 1, \dots, N \}.$$

The product space  $\mathcal{Z}_N = \mathcal{Z}_{\mathbf{v}}^{\chi} \times \mathcal{Z}_{\mathbf{h}}^{\lambda}$  can actually give a representation of the reduced state variable  $(\mathbf{v}_N(\boldsymbol{\mu}), h_N(\boldsymbol{\mu}))$  and the reduced adjoint variable  $(\chi_N(\boldsymbol{\mu}), \lambda_N(\boldsymbol{\mu}))$ . Moreover, setting  $\mathcal{Y}_N \equiv \mathcal{Q}_N \equiv \mathcal{Z}_N$ , the inf-sup condition (25) holds.

Concerning the control function space, a standard POD-procedure can be applied, building

$$\mathcal{U}_N = \text{span} \{ \zeta_n^{\mathbf{u}}, n = 1, \dots, N \}.$$

The aggregated space technique allows us to define new basis matrices of the form:

$Z_{\mathbf{v}} \equiv Z_{\chi} = [\zeta_1^{\mathbf{v}} | \dots | \zeta_N^{\mathbf{v}} | \zeta_1^{\chi} | \dots | \zeta_N^{\chi}] \in \mathbb{R}^{N_t N_v \times 2N}$ ,  $Z_{\mathbf{u}} = [\zeta_1^{\mathbf{u}} | \dots | \zeta_N^{\mathbf{u}}] \in \mathbb{R}^{N_t N_u \times N}$  and  $Z_{\mathbf{h}} \equiv Z_{\lambda} = [\zeta_1^{\mathbf{h}} | \dots | \zeta_N^{\mathbf{h}} | \zeta_1^{\lambda} | \dots | \zeta_N^{\lambda}] \in \mathbb{R}^{N_t N_h \times 2N}$ . The new spaces are actually increasing the dimension of the system since the global reduced dimension is  $N_{\text{tot}} = 9N$ . Although, the strategy guarantees the reduced inf-sup condition (25) and, consequently, the existence of an optimal solution. Still,  $N_{\text{tot}} < \mathcal{N}_{\text{tot}}$ , i.e. we still work in a reduced dimensional framework.

We introduced all the notions needed in order to reduce nonlinear time dependent OCP( $\boldsymbol{\mu}$ )s. Anyway, we still miss fundamental assumptions which allow ROM to be very advantageous under the point of view of computational costs, which will be the topic of the next Section.

### 3.4 Efficient ROM and Affinity Assumption: Offline–Online decomposition

Exploiting a reduced strategy is convenient only if fast simulations can be assured in order to analyse different configurations of the physical system for several parameters. To guarantee an efficient applicability of ROM techniques, the system is assumed to be affinely decomposed. In other words, all the quantities involved in the system have to be cast as the product of  $\boldsymbol{\mu}$ -dependent quantities and  $\boldsymbol{\mu}$ -independent quantities, i.e. the equations involved can be recast as:

$$\begin{aligned} D_{\mathbf{v}} \mathcal{L}((\mathbf{v}, h), \mathbf{u}, (\chi, \lambda))[z] &= \sum_{q=1}^{Q_{D_{\mathbf{v}} \mathcal{L}}} \Theta_{D_{\mathbf{v}} \mathcal{L}}^q(\boldsymbol{\mu}) D_{\mathbf{v}} \mathcal{L}^q((\mathbf{v}, h), \mathbf{u}, (\chi, \lambda))[z], \\ D_{\mathbf{h}} \mathcal{L}((\mathbf{v}, h), \mathbf{u}, (\chi, \lambda))[q] &= \sum_{q=1}^{Q_{D_{\mathbf{h}} \mathcal{L}}} \Theta_{D_{\mathbf{h}} \mathcal{L}}^q(\boldsymbol{\mu}) D_{\mathbf{h}} \mathcal{L}^q((\mathbf{v}, h), \mathbf{u}, (\chi, \lambda))[q], \\ D_{\mathbf{u}} \mathcal{L}((\mathbf{v}, h), \mathbf{u}, (\chi, \lambda))[\tau] &= \sum_{q=1}^{Q_{D_{\mathbf{u}} \mathcal{L}}} \Theta_{D_{\mathbf{u}} \mathcal{L}}^q(\boldsymbol{\mu}) D_{\mathbf{u}} \mathcal{L}^q((\mathbf{v}, h), \mathbf{u}, (\chi, \lambda))[\tau], \\ D_{\chi} \mathcal{L}((\mathbf{v}, h), \mathbf{u}, (\chi, \lambda))[\kappa] &= \sum_{q=1}^{Q_{D_{\chi} \mathcal{L}}} \Theta_{D_{\chi} \mathcal{L}}^q(\boldsymbol{\mu}) D_{\chi} \mathcal{L}^q((\mathbf{v}, h), \mathbf{u}, (\chi, \lambda))[\kappa], \\ D_{\lambda} \mathcal{L}((\mathbf{v}, h), \mathbf{u}, (\chi, \lambda))[\xi] &= \sum_{q=1}^{Q_{D_{\lambda} \mathcal{L}}} \Theta_{D_{\lambda} \mathcal{L}}^q(\boldsymbol{\mu}) D_{\lambda} \mathcal{L}^q((\mathbf{v}, h), \mathbf{u}, (\chi, \lambda))[\xi]. \end{aligned} \tag{26}$$

for some finite  $Q_{D_v\mathcal{L}}, Q_{D_h\mathcal{L}}, Q_{D_u\mathcal{L}}, Q_{D_\chi\mathcal{L}}, Q_{D_\lambda\mathcal{L}}$ , where  $\Theta_{D_v\mathcal{L}}^q, \Theta_{D_h\mathcal{L}}^q, \Theta_{D_u\mathcal{L}}^q, \Theta_{D_\chi\mathcal{L}}^q$  and  $\Theta_{D_\lambda\mathcal{L}}^q$  are  $\boldsymbol{\mu}$ -dependent smooth functions, whereas  $D_v\mathcal{L}^q((\mathbf{v}, h), \mathbf{u}, (\boldsymbol{\chi}, \lambda)), D_h\mathcal{L}^q((\mathbf{v}, h), \mathbf{u}, (\boldsymbol{\chi}, \lambda)), D_u\mathcal{L}^q((\mathbf{v}, h), \mathbf{u}, (\boldsymbol{\chi}, \lambda)), D_\chi\mathcal{L}^q((\mathbf{v}, h), \mathbf{u}, (\boldsymbol{\chi}, \lambda))$  are  $D_\lambda\mathcal{L}^q((\mathbf{v}, h), \mathbf{u}, (\boldsymbol{\chi}, \lambda))$  are  $\boldsymbol{\mu}$ -independent quantities describing the optimality system.

Thanks to affine decomposition, the solution of our OCP( $\boldsymbol{\mu}$ ) can be performed in two different steps: an **offline** stage which consists in assembling all the parameter dependent quantities, building the reduced function spaces and storing all the quantities mentioned; then, an **online** stage deals with all the  $\boldsymbol{\mu}$ -dependent quantities and solves the whole reduced system (20). The latter phase is performed at every new parameter evaluation and gives us information about physical configurations in a small amount of time since it does not depend on the discrete full order dimension  $N_{\text{tot}}$ .

We underline that the case of interest deals at most with only quadratically nonlinear terms, we can guarantee the affinity assumption storing the appropriate nonlinear terms in third order tensors. If the OCP( $\boldsymbol{\mu}$ ) does not fulfill the decomposition (26), the empirical interpolation method (EIM) can recover the assumption, see [10] or [27, Chapter 5] as references.

In the next Section, we are going to present some numerical results for a nonlinear time-dependent OCP( $\boldsymbol{\mu}$ ) governed by SWE equations, in order to assert the applicability of ROM for this complicated model, which can be of great interest for many application in natural sciences and engineering.

## 4 Numerical Results

This Section aims at validating the numerical performances of POD-Galerkin projection over nonlinear time dependent OCP( $\boldsymbol{\mu}$ ) governed by SWEs. We put in a parametrized optimal control framework the academic test case presented in [24]. The experiment can be read as an inverse problem on the forcing term, i.e. find the control variable, needed in order to have a desired velocity-height state profile. Given a parameter  $\boldsymbol{\mu} = [\mu_1, \mu_2, \mu_3]$  in the parametric space  $\mathcal{P} = (0.00001, 1.) \times (0.01, 0.5) \times (0.1, 1.)$ , we solved the optimality system (5) built through Lagrangian approach, in the fashion of optimize-then-discretize technique, over the water basin described by  $\Omega = (0, 10) \times (0, 10)$ . As we already discussed in Section 2.1, the flat bathymetry does not actually affect the system, so we used  $z_b = 0$ . We simulate our system evolution in the time interval  $(0, T)$  with  $T = 0.8\text{s}$ . The OCP( $\boldsymbol{\mu}$ ) simulates the spreading of a mass of water with an initial Gaussian distributed elevation and null initial velocity: i.e.

$$\mathbf{v}_0 = \mathbf{0}, \quad \text{and} \quad h_0 = 0.2(1 + 5e^{(-(x_1-5)^2-(x_2-5)^2+1)}),$$

where  $x_1$  and  $x_2$  are the spatial coordinates. Under a controlling forcing term representing wind action and bottom friction, we want our solution to be similar to  $(\mu_3\mathbf{v}_d, \mu_3h_d)$ , where  $(\mathbf{v}_d, h_d)$  is the solution of the uncontrolled state equation (1), with null initial velocity and initial elevation  $h_{d0} = 2e^{(-(x_1-5)^2-(x_2-5)^2+1)}$  and null forcing term  $\mathbf{u} = \mathbf{0}$ .

In Section 2.1, we already specified the diffusive and advective role of  $\mu_1$  and  $\mu_2$ . In Table 1 we report all the specifics of the experiment that we are going to describe. The goal of the presented optimal control problem is to make our solution  $(\mathbf{v}, h)$  the most similar to the desired above mentioned profile. Once again we underline that we work in a parametrized framework, i.e. the controlled solution changes for different values of  $\boldsymbol{\mu} \in \mathcal{P}$ . All the results we present are given by the parameter  $\boldsymbol{\mu} = (0.1, 0.5, 1.)$ . Following the FE discretization technique proposed in [?], we used linear polynomials for the truth approximation of all the variables, i.e.  $r_v = r_h = r_u = 1$ . With respect to time discretization, we divided the time interval with  $\Delta t = 0.1$ , which leads to a number of time steps  $N_t = 8$ . The problem solved is quite complex even with this small

amount of time steps. In any case,  $\Delta t$  can be reduced following iterative techniques exploited in [28, 29, 59, 60]. Although, for the sake of simplicity, we used a direct solver for the algebraic system (13). In the end, at the truth approximation level, we deal with a system of a total dimension  $\mathcal{N}_{\text{tot}} = N_t \times \mathcal{N} = 94'016$ . In order to build the reduced optimality system (20), we applied the partitioned POD-Galerkin approach presented in Section 3.2. First of all we built five correlation matrices with  $N_{\text{max}} = 100$  for all the variables, respectively. The choice of  $N_{\text{max}}$  deals with an increasing effort in solving the offline phase: indeed, the problem described has a huge computational effort both in time and storage memory exploited for the basis construction: time and memory needed drastically grow for large values of  $N_{\text{max}}$ . Although, the value we used gave us a reliable description of the solution manifold, in a feasible computational time.

Let us define the *basis number*  $N$ , i.e. the number of eigenvalues/eigenvectors retained from the correlation matrices compression process of the POD. For this test case, the basis functions were obtained choosing  $N = 30$ . The basis number considered allowed us to well describe the full order approximated system in the reduced framework, as the reader can notice from the average relative errors represented in Figure 2 with the following norms:

$$\int_0^T \|\mathbf{v}^{\mathcal{N}} - \mathbf{v}_N\|_{H^1}^2 dt, \quad \int_0^T \|h^{\mathcal{N}} - h_N\|_{L^2}^2 dt$$

$$\int_0^T \|\mathbf{u}^{\mathcal{N}} - \mathbf{u}_N\|_{L^2}^2 dt, \quad \int_0^T \|\chi^{\mathcal{N}} - \chi_N\|_{H^1}^2 dt, \quad \text{and} \quad \int_0^T \|\lambda^{\mathcal{N}} - \lambda_N\|_{L^2}^2 dt.$$

The errors is averaged over a testing set of 20 parameters uniformly distributed: as expected, it decreases with respect the basis number  $N$  reaching a minimum value of  $10^{-3}$  state and adjoint velocity and a value of  $10^{-4}$  for state and adjoint elevation together with the control variable. Moreover, the effectiveness of the reduced model can be understood also from the comparison between the FE solutions and the ROM solutions presented in Figures 5 and 7 for the velocity and elevation state at  $t = 0.2s, 0.4s, 0.6s, 0.8s$ , respectively. The ROM procedure leads to a good representation of the FE solutions for the different time instances considered. The same conclusions can be drawn for the adjoint variables for velocity and height in Figure 6 and 8, respectively. Figure 9 shows the comparison between ROM and FE control variable: also in this case the plots match for the time instances considered. As one can see, the adjoint velocity profiles have the same behaviour of the control variable scaled by the factor  $\alpha$ , as a consequence of the optimality equation (11). Furthermore, we can also observe how the OCP( $\mu$ ) actually changes the uncontrolled solutions shown in Figure 3 in order to reach a configuration more similar to the profile represented in Figure 4.

Let us analyse the computational time comparison between FE and ROM simulations. We refer to the *speedup index* behaviour: it represents how many reduced simulations can be performed in the time of one FE optimality system solve. The speedup depends very mildly on the value of  $N$ , and it is of the order of  $O(30)$  for  $N = 1, \dots, 30$ .

We remind that in order to guarantee the solvability of the reduced saddle point problem arising from the linearized system, we used aggregated space technique presented in Section 3.3: it increased the reduced dimension of the system to  $N_{\text{tot}} = 9N = 270$ . Anyway, the speedup index underlines that it is actually convenient to perform a projection even in this larger reduced space, since the whole optimality system is actually very complex to be solved at the FE level, most of all if many simulations are required in order to better study several parametric configurations. The next Section is dedicated to some comments and perspectives on improvements and future research focus with respect to the presented topic.

**Table 1:** Data for the OCP( $\mu$ ) governed by SWEs.

| Data                                      | Values  |
|---|---|
| $\mathcal{P}$                             | $(0.00001, 1) \times (0.01, 0.5) \times (0.1, 1)$ |
| $[0, T]$                                  | $[0s, 0.8s]$                                      |
| values of $(\mu_1, \mu_2, \mu_3, \alpha)$ | $(0.1, 0.5, 1, 10^{-1})$                          |
| $N_{\max}$                                | 100   |
| $N$                                       | 30  |
| Sampling Distribution                     | Uniform   |
| $\mathcal{N}_{\text{tot}}$                | 94'016  |
| ROM System Dimension                      | 270   |

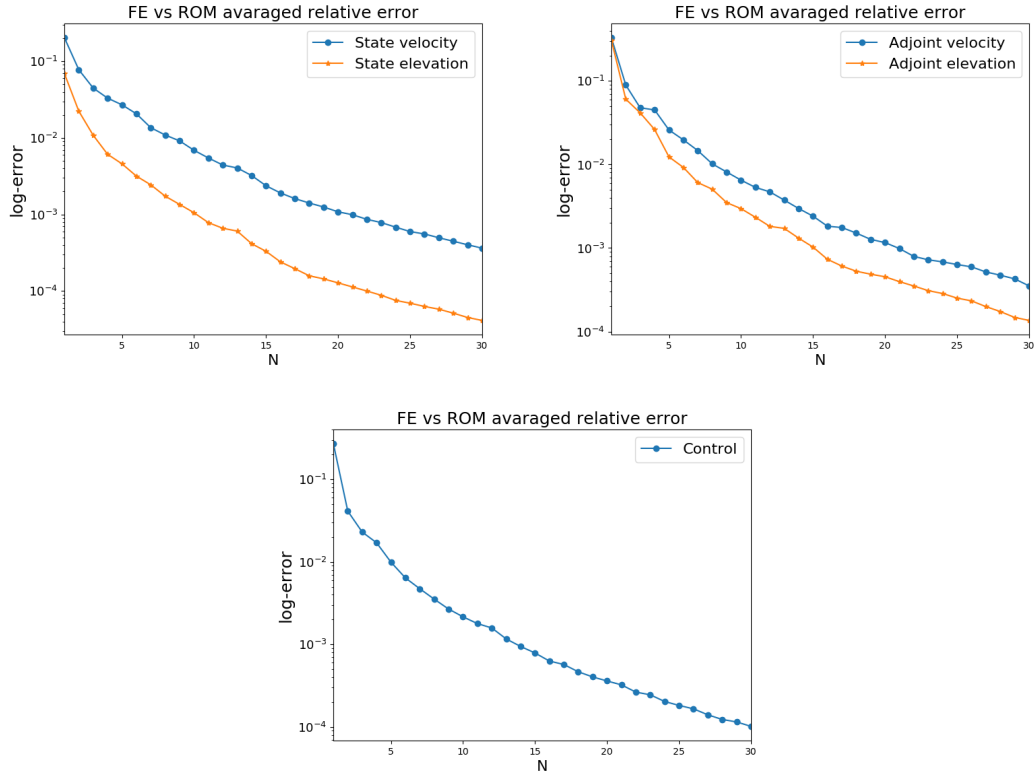


**Figure 2:** Averaged relative error between FE and ROM approximation for state velocity and elevation profile (top left), adjoint velocity and elevation profile (top right), and control (bottom).

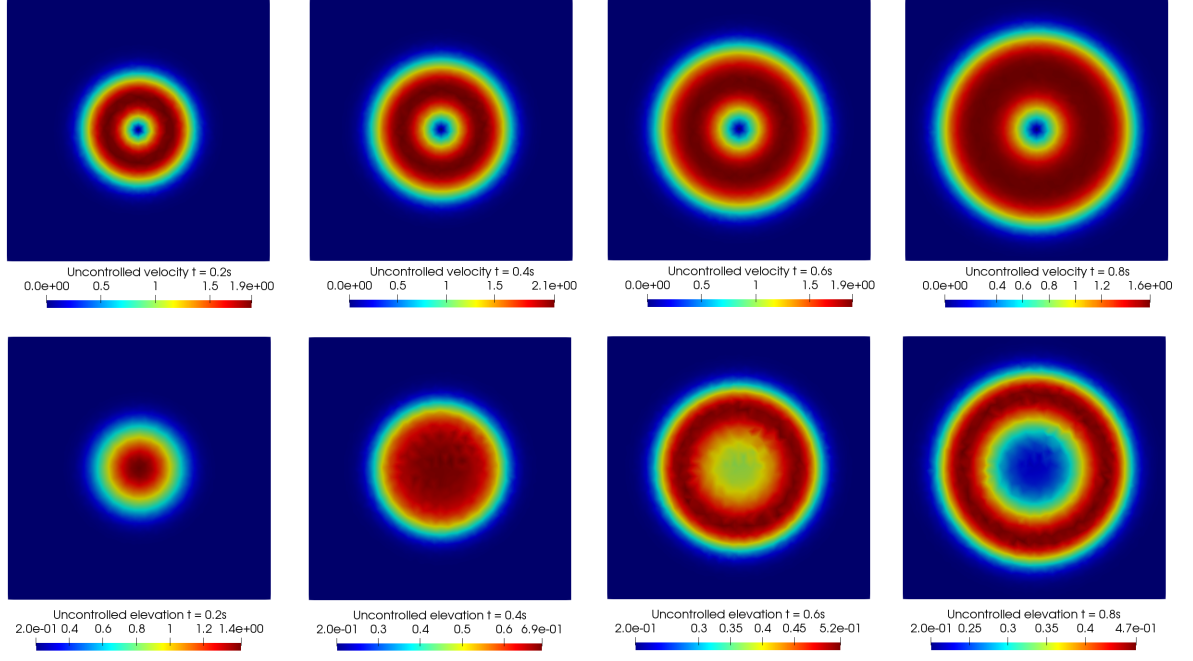


**Figure 3:** FE uncontrolled velocity (top) and elevation (bottom) for  $t = 0.2s, 0.4s, 0.6s, 0.8s$  and for  $\mu_1 = 0.1$  and  $\mu_2 = 0.5$ .

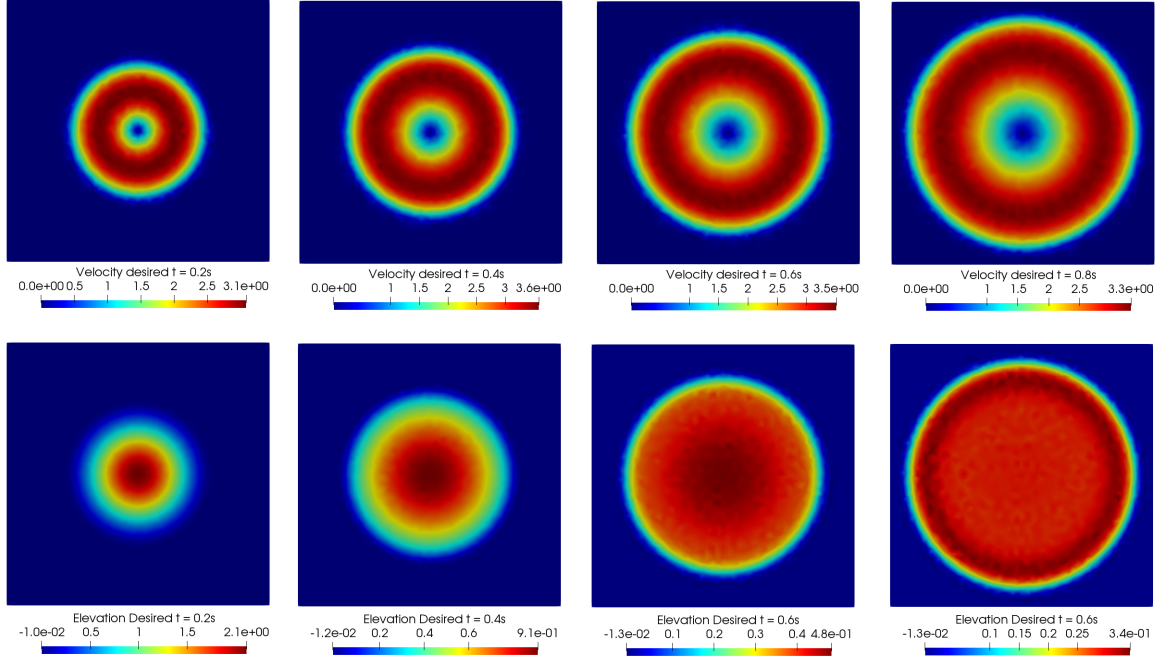


**Figure 4:** FE desired velocity (top) and elevation (bottom) for  $t = 0.2s, 0.4s, 0.6s, 0.8s$  and for  $\mu_1 = 0.0001$  and  $\mu_2 = 1$ .

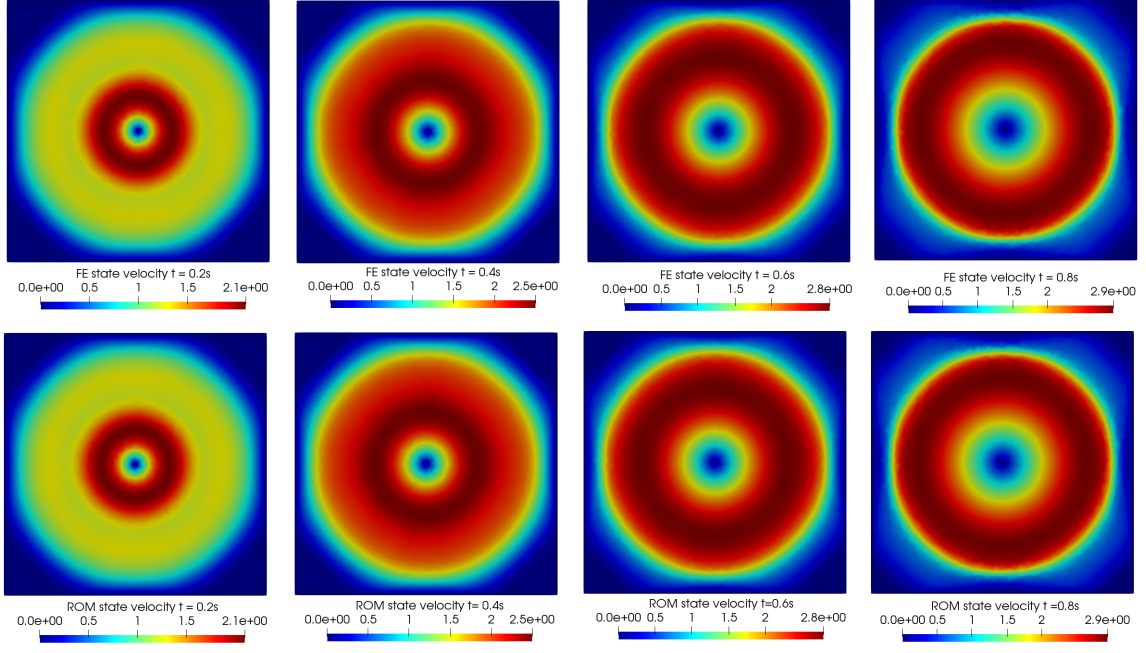


**Figure 5:** FE state velocity profile (top) compared to ROM state velocity profile (bottom) for  $t = 0.2s, 0.4s, 0.6s, 0.8s$  and for  $\mu = (0.1, 0.5, 1)$ .

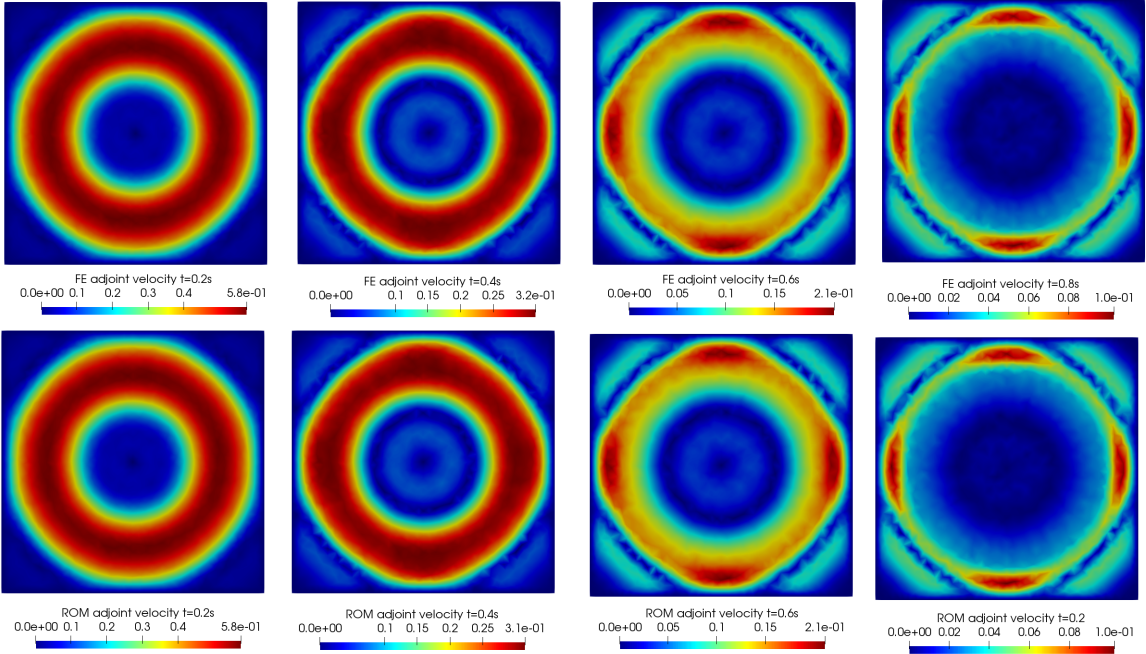


**Figure 6:** FE adjoint velocity profile (top) compared to ROM adjoint velocity profile (bottom) for  $t = 0.2s, 0.4s, 0.6s, 0.8s$  and for  $\mu = (0.1, 0.5, 1)$ .



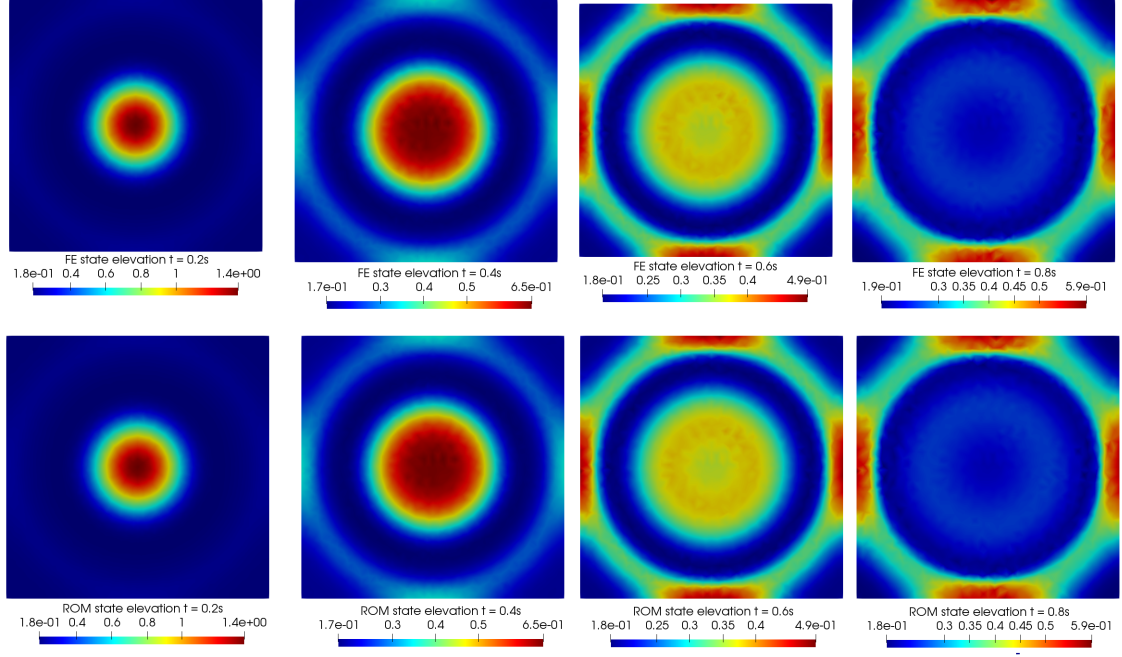


**Figure 7:** FE state elevation profile (top) compared to ROM state elevation profile (bottom) for  $t = 0.2s, 0.4s, 0.6s, 0.8s$  and for  $\mu = (0.1, 0.5, 1)$ .

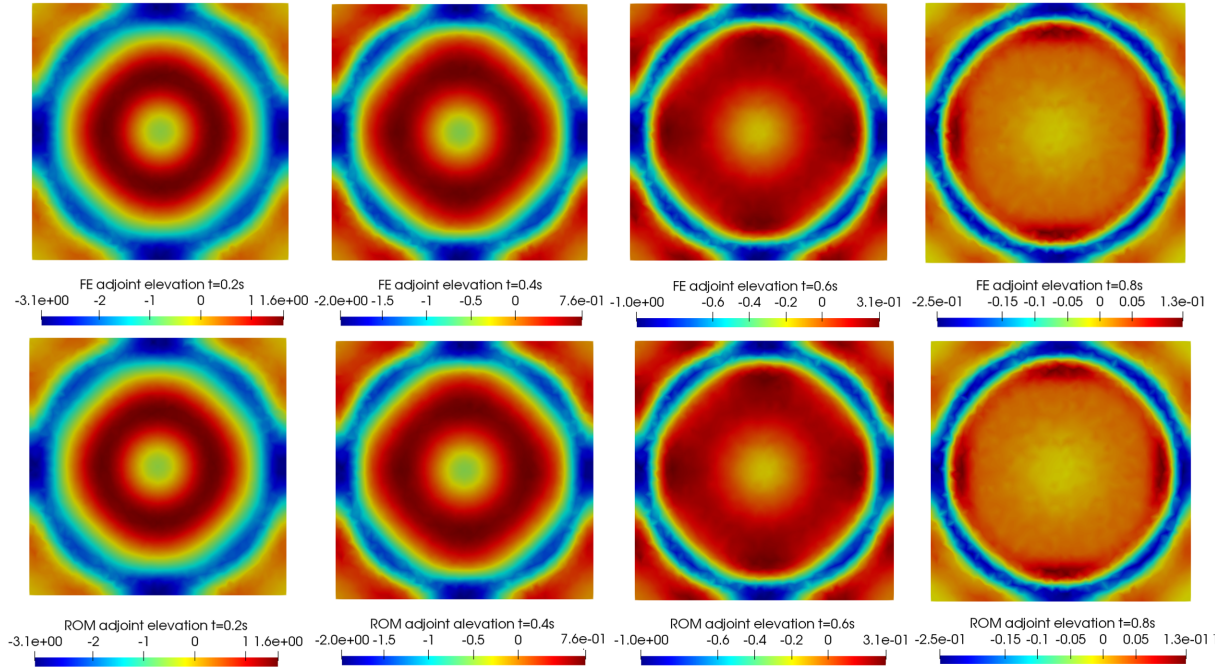


**Figure 8:** FE adjoint elevation profile (top) compared to ROM adjoint elevation profile (bottom) for  $t = 0.2s, 0.4s, 0.6s, 0.8s$  and for  $\mu = (0.1, 0.5, 1)$ .

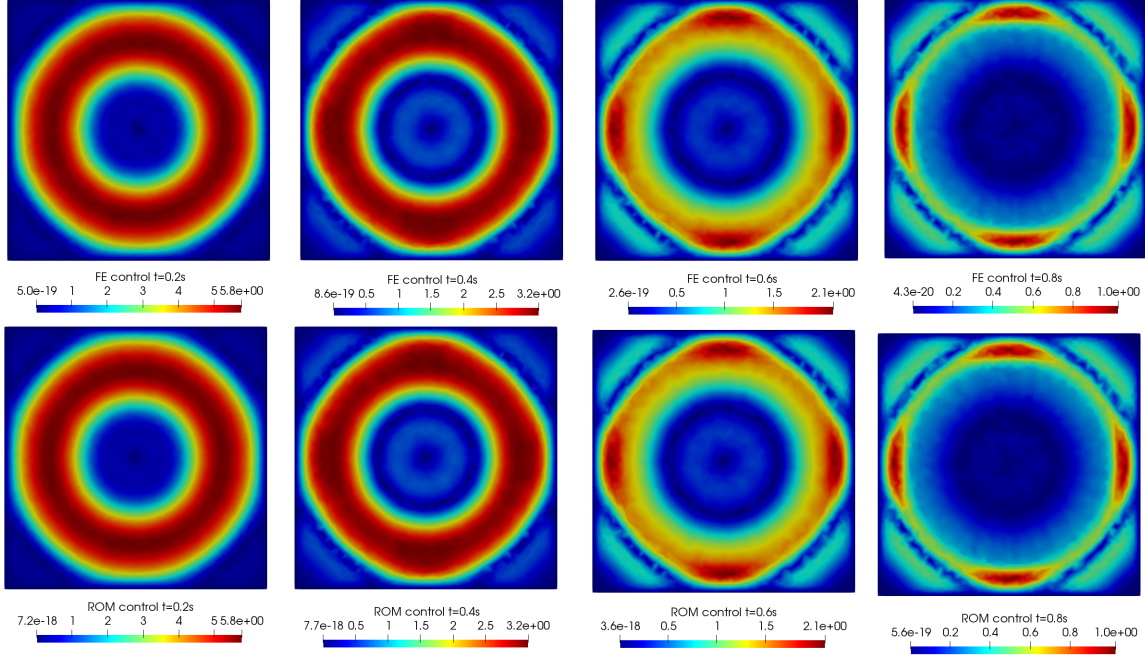


**Figure 9:** FE control variable (top) compared to ROM control variable (bottom) for  $t = 0.2s, 0.4s, 0.6s, 0.8s$  and for  $\mu = (0.1, 0.5, 1)$ .

## 5 Conclusion and Perspectives

In this work, we propose ROMs as a suitable tool to solve a parametrized nonlinear time dependent OCP( $\mu$ ) governed by SWE, a very important model widely spread in several environmental applications such as marine ecosystem management and coastal engineering. To the best of our knowledge, it is the first time that parametrized reduction is exploited for this kind of solution tracking coastal model: this work aims at showing how ROMs could be very effective in the marine management field deeply characterized by a growing demanding computational effort. Working in a low dimensional framework allows us to perform accurate simulations in a small amount of time compared to FE approximation. Moreover, the proposed methodology, based on a POD-Galerkin projection of the Lagrangian based optimality system, is general and can be applied to every nonlinear time dependent state equations. Indeed, a complete reduced data assimilated nonlinear and time dependent framework is presented and, since it can be used for general state equations, it can represent several environmental problem configurations.

Some possible advances to this work follow. First of all, a more theoretical analysis of the considered problem is still partially missing due to the great complexity of the state equation itself. The analysis of the parametrized optimal control framework governed by SWEs could be a topic of future investigation, as well as the development of an error estimator which could allow us to develop more efficient ROM greedy-based algorithms.

For environmental sciences applications, another important development for nonlinear time dependent problems could be the use of random input parameters as an extension of [17], since, in marine ecosystems, it is not always possible to assign deterministic values for the parameters describing the physical model.

## Acknowledgements

We acknowledge the support by European Union Funding for Research and Innovation – Horizon 2020 Program – in the framework of European Research Council Executive Agency: Consolidator Grant H2020 ERC CoG 2015 AROMA-CFD project 681447 “Advanced Reduced Order Methods with Applications in Computational Fluid Dynamics”. We also acknowledge the INDAM-GNCS project “Advanced intrusive and non-intrusive model order reduction techniques and applications” and the PRIN 2017 “Numerical Analysis for Full and Reduced Order Methods for the efficient and accurate solution of complex systems governed by Partial Differential Equations” (NA-FROM-PDEs). The computations in this work have been performed with RBniCS [1] library, developed at SISSA mathLab, which is an implementation in FEniCS [40] of several reduced order modelling techniques; we acknowledge developers and contributors to both libraries.

## References

- [1] RBniCS - reduced order modelling in FEniCS. <http://mathlab.sissa.it/rbnics>, 2015.
- [2] V Agoshkov, E Ovchinnikov, A Quarteroni, and F Saleri. Recent developments in the numerical simulation of shallow water equations II: Temporal discretization. *Mathematical Models and Methods in Applied Sciences*, 4(04):533–556, 1994.
- [3] V. I. Agoshkov, D. Ambrosi, V. Pennati, A. Quarteroni, and F. Saleri. Mathematical and numerical modelling of shallow water flow. *Computational Mechanics*, 11(5):280–299, Sep 1993.
- [4] V. I. Agoshkov, A. Quarteroni, and F. Saleri. Recent developments in the numerical simulation of shallow water equations I: Boundary conditions. *Applied Numerical Mathematics*, 15(2):175–200, 1994.
- [5] V. I. Agoshkov, F. Saleri, and E. Miglio. An optimal control approach for 1D-2D shallow water equations coupling. In *Communications to SIMAI Congress*, volume 1, 2007.
- [6] I. Babuška. Error-bounds for finite element method. *Numerische Mathematik*, 16(4):322–333, Jan 1971.
- [7] E. Bader, M. Kärcher, M. A. Grepl, and K. Veroy. Certified reduced basis methods for parametrized distributed elliptic optimal control problems with control constraints. *SIAM Journal on Scientific Computing*, 38(6):A3921–A3946, 2016.
- [8] E. Bader, M. Kärcher, M. A. Grepl, and K. Veroy-Grepl. A certified reduced basis approach for parametrized linear-quadratic optimal control problems with control constraints. *IFAC-PapersOnLine*, 48(1):719–720, 2015.
- [9] F. Ballarin, A. Manzoni, A. Quarteroni, and G. Rozza. Supremizer stabilization of POD–Galerkin approximation of parametrized steady incompressible Navier–Stokes equations. *International Journal for Numerical Methods in Engineering*, 102(5):1136–1161, 2015.
- [10] M. Barrault, Y. Maday, N. C. Nguyen, and A. T. Patera. An Empirical Interpolation Method: application to efficient reduced-basis discretization of partial differential equations. *Comptes Rendus Mathématique*, 339(9):667–672, 2004.

- [11] M. Benzi, G. H. Golub, and J. Liesen. Numerical solution of saddle point problems. *Acta Numerica*, 14:1–137, 2005.
- [12] P. B. Bochev and M. D. Gunzburger. *Least-squares finite element methods*, volume 166. Springer-Verlag, New York, 2009.
- [13] D. Boffi, F. Brezzi, and M. Fortin. *Mixed finite element methods and applications*, volume 44. Springer-Verlag, Berlin and Heidelberg, 2013.
- [14] J. Bramble, J. Pasciak, and A. Vassilev. Uzawa type algorithms for nonsymmetric saddle point problems. *Mathematics of Computation*, 69(230):667–689, 2000.
- [15] F. Brezzi. On the existence, uniqueness and approximation of saddle-point problems arising from lagrangian multipliers. *ESAIM: Mathematical Modelling and Numerical Analysis - Modélisation Mathématique et Analyse Numérique*, 8(R2):129–151, 1974.
- [16] J. Burkardt, M. Gunzburger, and H.C. Lee. POD and CVT-based reduced-order modeling of Navier–Stokes flows. *Computer Methods in Applied Mechanics and Engineering*, 196(1-3):337–355, 2006.
- [17] G. Carere, M. Strazzullo, and G. Rozza. Weighted POD-reduction for parametrized optimal control problems with random inputs applied to environmental sciences. In preparation, 2020.
- [18] F. Cavallini and F. Crisciani. *Quasi-geostrophic theory of Oceans and atmosphere: topics in the dynamics and thermodynamics of the Fluid Earth*, volume 45. Springer Science & Business Media, New York, 2013.
- [19] D. Chapelle, A. Gariah, P. Moireau, and J. Sainte-Marie. A Galerkin strategy with proper orthogonal decomposition for parameter-dependent problems: Analysis, assessments and applications to parameter estimation. *ESAIM: Mathematical Modelling and Numerical Analysis*, 47(6):1821–1843, 2013.
- [20] L. Dedè. Reduced basis method and a posteriori error estimation for parametrized linear-quadratic optimal control problems. *SIAM Journal on Scientific Computing*, 32(2):997–1019, 2010.
- [21] L. Dedè. Adaptive and reduced basis method for optimal control problems in environmental applications. PhD thesis, Politecnico di Milano, 2008. Available at <http://mox.polimi.it>.
- [22] K. Eriksson and C. Johnson. Error estimates and automatic time step control for nonlinear parabolic problems, I. *SIAM Journal on Numerical Analysis*, 24(1):12–23, 1987.
- [23] E. Fernández Cara and E. Zuazua. Control theory: History, mathematical achievements and perspectives. *Boletín de la Sociedad Española de Matemática Aplicada*, 26, 79–140., 2003.
- [24] S. Ferrari and F. Saleri. A new two-dimensional shallow water model including pressure effects and slow varying bottom topography. *ESAIM: Mathematical Modelling and Numerical Analysis*, 38(2):211–234, 2004.
- [25] A. L. Gerner and K. Veroy. Certified reduced basis methods for parametrized saddle point problems. *SIAM Journal on Scientific Computing*, 34(5):A2812–A2836, 2012.

- [26] M. Ghil and P. Malanotte-Rizzoli. Data assimilation in meteorology and oceanography. *Advances in geophysics*, 33:141–266, 1991.
- [27] J. S. Hesthaven, G. Rozza, and B. Stamm. Certified reduced basis methods for parametrized partial differential equations. *SpringerBriefs in Mathematics*, 2015, Springer, Milano.
- [28] M.L. Hinze, M. Köster, and S. Turek. A hierarchical space-time solver for distributed control of the Stokes equation. *Technical Report, SPP1253-16-01*, 2008.
- [29] M.L. Hinze, M. Köster, and S. Turek. A space-time multigrid method for optimal flow control. In *Constrained optimization and optimal control for partial differential equations*, pages 147–170. Springer, 2012.
- [30] M.L. Hinze, R. Pinnau, M. Ulbrich, and S. Ulbrich. *Optimization with PDE constraints*, volume 23. Springer Science & Business Media, Antwerp, 2008.
- [31] L. Iapichino, S. Trenz, and S. Volkwein. Reduced-order multiobjective optimal control of semilinear parabolic problems. In Bülent Karasözen, Murat Manguoğlu, Münevver Tezer-Sezgin, Serdar Göktepe, and Ömür Uğur, editors, *Numerical Mathematics and Advanced Applications ENUMATH 2015*, pages 389–397, Cham, 2016. Springer International Publishing.
- [32] K. Ito and S. Ravindran. A reduced-order method for simulation and control of fluid flows. *Journal of computational physics*, 143(2):403–425, 1998.
- [33] E. Kalnay. *Atmospheric modeling, data assimilation and predictability*. Cambridge university press, 2003, Cambridge.
- [34] M. Kärcher and M. A. Grepl. A certified reduced basis method for parametrized elliptic optimal control problems. *ESAIM: Control, Optimisation and Calculus of Variations*, 20(2):416–441, 2014.
- [35] M. Kärcher and M. A. Grepl. A posteriori error estimation for reduced order solutions of parametrized parabolic optimal control problems. *ESAIM: Mathematical Modelling and Numerical Analysis*, 48(6):1615–1638, 2014.
- [36] M. Kärcher, Z. Tokoutsi, M. A. Grepl, and K. Veroy. Certified reduced basis methods for parametrized elliptic optimal control problems with distributed controls. *Journal of Scientific Computing*, 75(1):276–307, 2018.
- [37] K. Kunisch and S. Volkwein. Proper orthogonal decomposition for optimality systems. *ESAIM: Mathematical Modelling and Numerical Analysis*, 42(1):1–23, 2008.
- [38] T. Lassila, A. Manzoni, A. Quarteroni, and G. Rozza. A reduced computational and geometrical framework for inverse problems in hemodynamics. *International Journal for Numerical Methods in Biomedical Engineering*, 29(7):741–776, 2013.
- [39] G. Leugering, P. Benner, S. Engell, A. Griewank, H. Harbrecht, M. Hinze, R. Rannacher, and S. Ulbrich. *Trends in PDE constrained optimization*. Springer, New York, 2014.
- [40] A. Logg, K.A. Mardal, and G. Wells. *Automated Solution of Differential Equations by the Finite Element Method*. Springer-Verlag, Berlin, 2012.
- [41] A. Manzoni, A. Quarteroni, and S. Salsa. Mox-report no . 13 / 2019. A saddle point approach to an optimal boundary control problem for steady Navier-Stokes equations. 2019.

- [42] E. Miglio, S. Perotto, and F. Saleri. Model coupling techniques for free-surface flow problems: Part I. *Nonlinear Analysis: Theory, Methods & Applications*, 63(5-7):e1885–e1896, 2005.
- [43] E. Miglio, S. Perotto, and F. Saleri. Model coupling techniques for free-surface flow problems: Part II. *Nonlinear Analysis: Theory, Methods & Applications*, 63(5-7):e1897–e1908, 2005.
- [44] E. Miglio, A. Quarteroni, and F. Saleri. Finite element approximation of quasi-3D shallow water equations. *Computer Methods in Applied Mechanics and Engineering*, 174(3-4):355–369, 1999.
- [45] R. Mosetti, C. Fanara, M. Spoto, and E. Vinzi. Innovative strategies for marine protected areas monitoring: the experience of the Istituto Nazionale di Oceanografia e di Geofisica Sperimentale in the Natural Marine Reserve of Miramare, Trieste-Italy. In *OCEANS, 2005. Proceedings of MTS/IEEE*, pages 92–97. IEEE, 2005.
- [46] F. Negri, A. Manzoni, and G. Rozza. Reduced basis approximation of parametrized optimal flow control problems for the Stokes equations. *Computers & Mathematics with Applications*, 69(4):319–336, 2015.
- [47] F. Negri, G. Rozza, A. Manzoni, and A. Quarteroni. Reduced basis method for parametrized elliptic optimal control problems. *SIAM Journal on Scientific Computing*, 35(5):A2316–A2340, 2013.
- [48] C. Prud’Homme, D. V. Rovas, K. Veroy, L. Machiels, Y. Maday, A. Patera, and G. Turinici. Reliable real-time solution of parametrized partial differential equations: Reduced-basis output bound methods. *Journal of Fluids Engineering*, 124(1):70–80, 2002.
- [49] A. Quarteroni, G. Rozza, L. Dedè, and A. Quaini. Numerical approximation of a control problem for advection-diffusion processes. In *Ceragioli F., Dontchev A., Futura H., Marti K., Pandolfi L. (eds) System Modeling and Optimization. International Federation for Information Processing, CSMO Conference on System Modeling and Optimization*, pages vol 199, 261–273. Springer, Boston, 2005.
- [50] A. Quarteroni, G. Rozza, and A. Quaini. Reduced basis methods for optimal control of advection-diffusion problems. In *Advances in Numerical Mathematics*, number CMCS-CONF-2006-003, pages 193–216. RAS and University of Houston, 2007.
- [51] M. Ricchiuto, R. Abgrall, and H. Deconinck. Application of conservative residual distribution schemes to the solution of the shallow water equations on unstructured meshes. *Journal of Computational Physics*, 222(1):287–331, 2007.
- [52] M. Ricchiuto and A. Bollermann. Stabilized residual distribution for shallow water simulations. *Journal of Computational Physics*, 228(4):1071–1115, 2009.
- [53] G. Rozza, D.B.P. Huynh, and A.T. Patera. Reduced basis approximation and a posteriori error estimation for affinely parametrized elliptic coercive partial differential equations: Application to transport and continuum mechanics. *Archives of Computational Methods in Engineering*, 15(3):229–275, 2008.
- [54] G. Rozza, A. Manzoni, and F. Negri. Reduction strategies for PDE-constrained optimization problems in Haemodynamics. pages 1749–1768, ECCOMAS, September 2012, Congress Proceedings, Vienna, Austria.

- [55] G. Rozza and K. Veroy. On the stability of the reduced basis method for Stokes equations in parametrized domains. *Computer Methods in Applied Mechanics and Engineering*, 196(7):1244–1260, 2007.
- [56] T. Shiganova and A. Malej. Native and non-native ctenophores in the Gulf of Trieste, Northern Adriatic Sea. *Journal of Plankton Research*, 31(1):61–71, 11 2008.
- [57] R. Ștefănescu and I. M. Navon. POD/DEIM nonlinear model order reduction of an ADI implicit shallow water equations model. *Journal of Computational Physics*, 237:95–114, 2013.
- [58] R. Ștefănescu, A. Sandu, and I. M. Navon. Comparison of POD reduced order strategies for the nonlinear 2D shallow water equations. *International Journal for Numerical Methods in Fluids*, 76(8):497–521, 2014.
- [59] M. Stoll and A. Wathen. All-at-once solution of time-dependent PDE-constrained optimization problems. 2010.
- [60] M. Stoll and A. Wathen. All-at-once solution of time-dependent Stokes control. *J. Comput. Phys.*, 232(1):498–515, January 2013.
- [61] M. Strazzullo, F. Ballarin, R. Mosetti, and G. Rozza. Model reduction for parametrized optimal control problems in environmental marine sciences and engineering. *SIAM Journal on Scientific Computing*, 40(4):B1055–B1079, 2018.
- [62] M. Strazzullo, F. Ballarin, and G. Rozza. POD-galerkin model order reduction for parametrized time dependent linear quadratic optimal control problems in saddle point formulation. submitted, <https://arxiv.org/abs/1909.09631>, 2019.
- [63] M. Strazzullo, Z. Zainib, F. Ballarin, and G. Rozza. Reduced order methods for parametrized nonlinear and time dependent optimal flow control problems: towards applications in biomedical and environmental sciences. Submitted, <https://arxiv.org/abs/1912.07886>, 2019.
- [64] S. Takase, K. Kashiwayama, S. Tanaka, and T. E. Tezduyar. Space–time SUPG formulation of the shallow-water equations. *International Journal for Numerical Methods in Fluids*, 64(10-12):1379–1394, 2010.
- [65] F. Tröltzsch. Optimal control of partial differential equations. *Graduate studies in mathematics*, 112, Verlag, Wiesbad, 2010.
- [66] E. Tziperman and W. C. Thacker. An optimal-control/adjoint-equations approach to studying the Oceanic general circulation. *Journal of Physical Oceanography*, 19(10):1471–1485, 1989.
- [67] K. Urban and A. T. Patera. A new error bound for reduced basis approximation of parabolic partial differential equations. *Comptes Rendus Mathématique*, 350(3-4):203–207, 2012.
- [68] C. B. Vreugdenhil. *Numerical methods for shallow-water flow*, volume 13. Springer Science & Business Media, 2013.
- [69] M. Yano. A space-time Petrov–Galerkin certified reduced basis method: Application to the Boussinesq equations. *SIAM Journal on Scientific Computing*, 36(1):A232–A266, 2014.

- [70] M. Yano, A. T. Patera, and K. Urban. A space-time hp-interpolation-based certified reduced basis method for Burgers' equation. *Mathematical Models and Methods in Applied Sciences*, 24(09):1903–1935, 2014.
- [71] Z. Zainib, F. Ballarin, G. Rozza, P. Triverio, L. Jiménez-Juan, and S. Frenes. Reduced order methods for parametric optimal flow control in coronary bypass grafts, towards patient-specific data assimilation. Submitted, <https://arxiv.org/abs/1911.01409>, 2019.